Structural Fire Engineering Research Today and Tomorrow

Pettersson, Ove

1966

LUND INSTITUTE OF TECHNOLOGY · LUND · SWEDEN · 1966
DIVISION OF STRUCTURAL MECHANICS AND CONCRETE CONSTRUCTION - BULLETIN 1

OVE PETTERSSON

STRUCTURAL FIRE ENGINEERING RESEARCH TODAY AND TOMORROW

Ci 33

UDC 699.81.001.5:614.841.33

ACTA POLYTECHNICA SCANDINAVICA

CIVIL ENGINEERING AND BUILDING CONSTRUCTION
SERIES No. 33

Structural Fire Engineering Research Today and Tomorrow

Ove Pettersson

Lund Institute of Technology
Lund, Sweden
National Swedish Institute for Materials Testing
Stockholm, Sweden

STOCKHOLM 1965

PRINTED IN SWEDEN BY
ELANDERS BOKTRYCKERI AKTIEBOLAG, GÖTEBORG 1965

Preface

The field of structural fire engineering research is a typical borderline region, in which substantial scientific contributions usually presuppose thorough familiarity with many branches of mathematics, natural science, and engineering. Research fields of this type have often been treated in a relatively negligent manner, and structural fire engineering is unfortunately no exception in this respect.

Fire engineering design of buildings and parts of buildings is at present characterised by procedures which are non-functional and undifferentiated from the viewpoint of structural design, and which are to a great extent based on regulations and recommendations. For instance, load-bearing structures are nowadays conventionally designed in a comparatively judicious fashion so as to take account of static and dynamic loads, whereas the state of fire engineering design gives rise to an undesirable lack of balance between these two fundamental and equivalent phases of structural design work.

The object of this publication is to evolve a theoretical procedure of structural fire engineering design which is intended to be qualitatively equivalent to the present-day methods of design for static and dynamic loads. The various steps of the design procedure in question are dealt with in detail, and are illustrated by examples which spotlight the scope of knowledge that is available in this field today. In this connection, mention is also made of the most important research problems which must be solved in order that the proposed procedure may be applied as generally as possible in the future.

The present publication, which is an elaboration of the paper that appeared in the Swedish review "Gullkornet" under the title "Den byggnadstekniska brandforskningen i dag och i framtiden" (Structural Fire Engineering Research Today and Tomorrow) in 1964, is to be regarded as a complement to the "General Programme for Scandinavian Long-Term Fire Engineering Research", see Reference [72], which has been drawn up by the Author in the spring of 1963 at the request of the Inter-Scandinavian Liaison Group (Nordiska Samarbetsgruppen, abbreviated NS) for Inter-Scandinavian Building Research Conferences (Nordiska Byggforskningsmöten, abbreviated NBM), of the Liaison Committee of Scandinavian Fire Prevention Laboratories (Nordiska Brandlaboratoriernas Samarbetskommitté, abbreviated NBS), and of the National Swedish Institute for Materials Testing, Stockholm.

The Author wishes to express his hearty thanks to Mr. Ilya Cyon, who translated the manuscript into English, and to Miss Birgitta Andersson, who prepared the drawings for publication.

Lund and Stockholm, December 1965

Ove Pettersson

Table of Contents

Introduction

Structural fire engineering research occupies today a markedly subordinate position in the engineering research sector. The literature in this field has so far exhibited two outstanding characteristics. First, theoretical studies of this subject are extremely scanty. Second, as regards experimental research, it is to be noted that the major part of the investigations published at both national and international levels are primarily to be qualified as limited tests, from which some fundamental data that are peculiar to the material under test or to the structure under test can be derived, but from which, on the other hand, no generally applicable conclusions can be drawn.

As a consequence of the situation outlined in the above, our specialised knowledge in the field of structural fire engineering is at present highly unsatisfactory. This state of affairs gives rise to extraordinary difficulties in the design of buildings or parts of buildings with a view to ensuring that they shall be structurally and functionally well-defined and correctly well-adapted from a fire engineering point of view. These difficulties manifest themselves perhaps most strikingly in connection with the load-bearing structures, which are nowadays normally designed in a judicious and thorough manner so as to take account of static and dynamic loads, whereas their design with reference to fire resistance is dealt with in an extremely stereotyped way on the basis of lists which are founded on experience, and which specify the fire resistance in terms of time under standard fire conditions for structures and structural members of commonly used types. It is evident that such an unbalance between these two basic and equivalent aspects of design is an unquestionably serious drawback, which must be obviated as soon as possible, and the only practicable means of gaining this end is to be found in actively intensified, systematic long-term research and development work in the structural engineering field.

Some of the structural fire engineering problems which are essential in this research and development work will be summarily discussed in what follows. At the same time, some fragmentary comments on the present state of knowledge in the allied fields will be made along with the discussion of these problems. In order that the subject under consideration may be treated within a reasonable space, it has been decided that the scope of this paper should be confined to the main problems met with in the fire engineering design of load-bearing structures.

1. Principles of Fire Engineering Design of Load-Bearing Structures [1][1])

The problem of designing load-bearing structures or structural members with reference to their fire resistance is essentially an economic minimum problem in which it is required to minimise the sum of the cost of fire-fighting services, the cost of fire prevention, and the probable cost of damage due to fire. The last-mentioned cost is defined as the sum of the products of the probability of damage multiplied by the cost of damage for all types of damage which can be caused by fire to the structure under consideration. The first two of the above-mentioned three cost factors can nowadays be estimated in advance with satisfactory accuracy, while the requisite basic data for estimating beforehand the probable cost of damage due to fire are for the most part not available at the present time. An enormous amount of work is necessary in order to collect these data, and it may therefore be presumed to be unrealistic to expect that structural design with reference to fire resistance on the basis of a minimum total cost can be put into practice to any appreciable extent in the next decades.

These circumstances make it necessary to simplify the problem under consideration. A natural and reasonable object of such a simplification is the requirement that the fire engineering design should be carried out in conformity with the fundamental principles which are conventionally used at the present time in the static design of load-bearing structures. Stated in a summary manner, this requirement implies that the temperature distribution in the structure or the structural member, and the corresponding minimum load-bearing capacity, which shall exceed by a stipulated safety margin the value referred to the static load, must be calculated on the basis of the quantity of combustible material (fire load) met with in each individual case. Unfortunately, even the basic data required for such a simplified method of fire engineering design have been studied so little that they are at present altogether inadequate. It is for this reason that we are forced by necessity to reconcile ourselves with the fact that the approach to fire engineering design, such as it is today, has to be extremely schematic, as it is characterised by procedures which consistently suppress genuine constructive thought, and which are wholly governed by compliance with regulations and recommendations.

[1]) The figures in brackets indicate the literature references at the end of this paper.

In order that it may be possible to evolve practically applicable methods of fire engineering design which are framed so as to be equivalent in set-up to the present-day conventional procedures used in the static design of load-bearing structures, it is necessary to undertake research with a view to solving the following main problems

(a) To determine the magnitude of the fire load in buildings of the types which are commonly met with in practice.

(b) To study the process of fire development in enclosed spaces, as influenced by varying properties of the combustible material as well as by those of the enclosing walls, floors, and ceilings.

(c) To investigate the thermal properties of common structural materials within the whole temperature range to be considered in connection with fires.

(d) To explore the effects of the fire temperature on the strength and deformation characteristics of common structural materials.

(e) To devise methods, simplified so far as possible, for calculating temperature fields in structures under unsteady-state conditions of heat transmission.

(f) To evolve methods which enable the load-bearing capacity of load-bearing structures exposed to fires to be calculated on the basis of the data obtained under (d) and (e).

Comments on these main problems will be found in the following sections.

2. Fire Loads

A survey of the fire loads which are met with in buildings of the most common types must be carried out on a broad statistical basis in order to provide a reliable foundation for realistic estimates of the requirements which should be stipulated from a fire engineering point of view for a structure or a structural member in each individual case.

The fire load constitutes a measure of the total quantity of combustible materials that is present in an enclosed room (this quantity includes the structural frame, the fixtures and furnishings, as well as the wall and ceiling finishes, and the floor covering). In the regulations and recommendations which are applied in various countries, the fire load is ordinarily stated in terms of an equivalent average quantity of wood, which is expressed in kilogrammes per square metre of floor area. This way of stating the fire load is inappropriate in that the quantity defined as the amount of fuel per unit floor area has no physical meaning as a parameter that is characteristic of a process of fire development. On the other hand, if this quantity is modified so as to express the amount of fuel per unit area of the total surface bounding the enclosed room, then we obtain a parameter which has a real physical significance. Accordingly, it is natural and important that this parameter should soon be adopted as a characteristic of fire loads in enclosed spaces [2].

With a view to long-range objectives, it is furthermore imperative that the fire load should be described in a manner that is more differentiated from a combustion standpoint. It seems that a practical procedure in achieving this purpose would be to state the heat value (calorific value) of the fire load per unit area of the total surface bounding an enclosed space, and to specify the frequency curve of the rates of combustion which correspond to the various components of this heat value, and which should be referred to strictly defined conditions of combustion, e.g. open fires in air having definite pressure, temperature, and relative humidity characteristics. It is moreover essential to show at the same time the frequency curve of those emissivities of the flames and smoulders associated with a fire which correspond to the different components of the heat value.

The extensive statistical basis which is required in order that differentiated regulations and recommendations for fire loads in common building structures may be drawn up in accordance with the general principles outlined in the above is almost entirely non-existent today. In the present situation, our

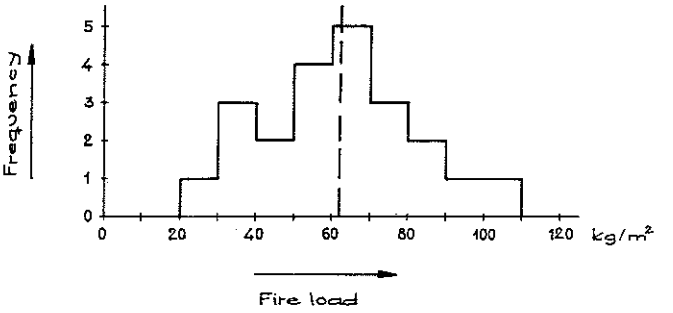

Fig. 1. Frequency curve of fire loads determined in Japanese office buildings with concrete load-bearing structures. Mean value=62, standard deviation=10,2 kg of equivalent amount of wood per square metre of floor area [3].

knowledge in this field is everywhere limited to a quantity that is inappropriate from a combustion engineering point of view, namely, the heat value per unit floor area, which is ordinarily expressed in kilogrammes of wood per square metre. The statistical basis which is nowadays available for estimating this quantity varies greatly in extent from one country to another. In most countries, including Scandinavia, the relevant statistical data are manifestly incomplete, whereas the literature in some other countries, particularly in Japan, contains relatively extensive results obtained from surveys which have been carried out systematically in order to determine the fire loads in buildings of the most common types. This is exemplified in Table 1 by the values of fire loads which are characteristic of Japanese buildings with concrete load-bearing structures and in Fig. 1, which shows the associated statistical frequency curve of fire loads in office buildings.

When the values of fire loads which have been statistically determined in one country are to be applied in other countries, this may meet with difficulties due to differences in types of buildings and in ways of life. A striking illustration of these difficulties may be provided by a comparison between the fire load values represented in Fig. 1, which are characteristic of Japanese office buildings, and the results of a very extensive survey made in modern Swiss offices in order to determine the corresponding fire load values, which were all found to be comprised in the range from 8 to 25 kg of wood per m^2 of floor area [4]. However, in making such a comparison, it is necessary to take account of the differences which arise when a fire load, in kilogrammes of wood, is converted to a heat value, in kilogramme-calories. For this conversion. the Swiss use a heat value of 4000 kcal per kg, whereas the Japanese

Table 1. Fire loads in Japanese buildings with concrete load-bearing structures

Type of building	Fire load, kg of wood per m^2 of floor area
Apartments	40 to 70
Hospitals	30 to 60
Hotels	25 to 40
Offices	30 to 150
Classrooms in schools	20 to 50
Libraries	300 to 600
Libraries (reading rooms only)	50 to 350
Warehouses	50 to 200
Department stores	20 to 75

utilise a considerably lower value of 2575 kcal per kg, which corresponds to a degree of combustion of only about 60 per cent.

To sum up the above considerations on fire loads, it may be stated that the present standing of knowledge in this field is markedly inadequate. In particular, the scope of this knowledge is insufficient for a differentiated characterisation of fire loads in conformity with the general principles expounded in the above, which recommend that the heat value per unit area of the total surface bounding an enclosed space should be specified, together with the corresponding frequency curves of the rates of combustion and the emissivities under well-defined conditions of combustion. With a view to drawing up future regulations and recommendations, it is therefore extremely important that statistical surveys should be started without delay for the purpose of determining as accurately as possible the characteristics of fire loads in buildings of the most common types. These surveys should be carried out on such a scale that the statistical data collected in this way make it possible to calculate the mean value of the fire load, the standard deviation in this load, and preferably also the type of the statistical distribution curve of fire loads with an accuracy that is acceptable under practical conditions.

3. Process of Fire Development

In the regulations and recommendations which are in force in various countries, the process of fire development in enclosed rooms is characterised by standard temperature-time curves, which are based on the assumption that the amount of fuel in the enclosed space is unlimited, see Fig. 2. On the other hand, if the amount of fuel in an enclosed space is limited, then it is assumed that the temperature-time relation is represented by the standard curve up to a certain definite instant, which is determined by the amount of fuel or the fire load, see Fig. 3. After this instant, the temperature in the enclosed space is supposed to decrease to ordinary room temperature either instantaneously

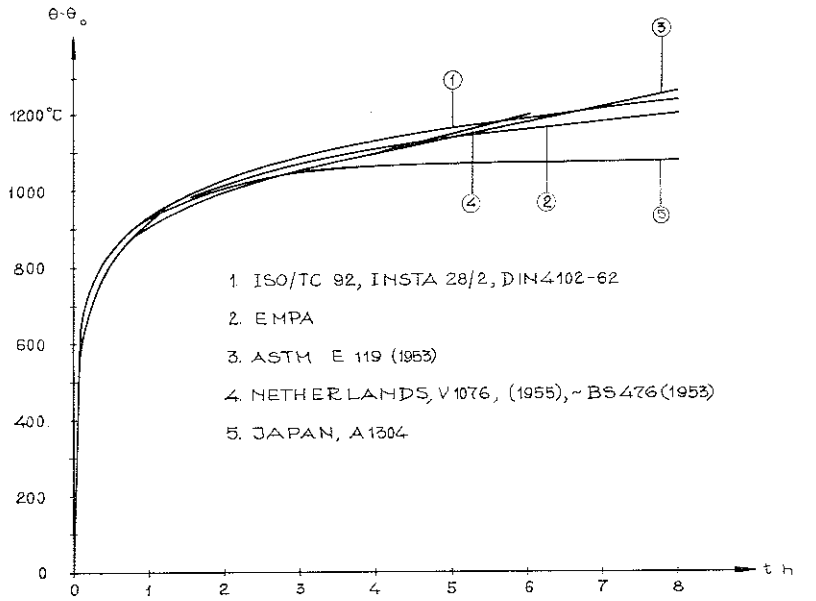

Fig. 2. Some standard curves used in various countries to represent the relation between the fire temperature, θ, and the time, t. These curves relate to enclosed spaces. θ_0 is the temperature in the enclosed space at the time $t=0$.

Curve 1: ISO/TC 92, INSTA 28/2, DIN 4102−62.
Curve 2: EMPA.
Curve 3: ASTM E 119 (1953).
Curve 4: Netherlands, V 1076 (1955). Approximately the same as B. S. 476 (1953).
Curve 5: Japan, A 1304.

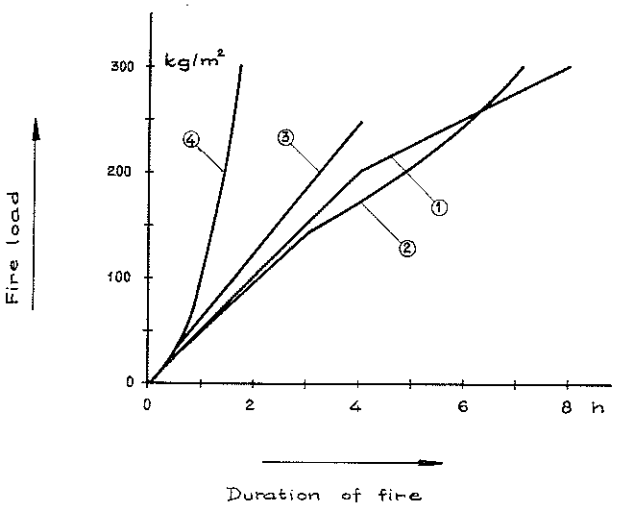

Fig. 3. Standard curves representing the relation between the fire load, in kilogrammes of wood per square metre of floor area, and the duration of the fire, in hours. These curves relate to enclosed spaces. Curve 1: Sweden. Curve 2: U.S.A. Curve 3: U.K. Curve 4: Swiss draft standard [5] to [8].

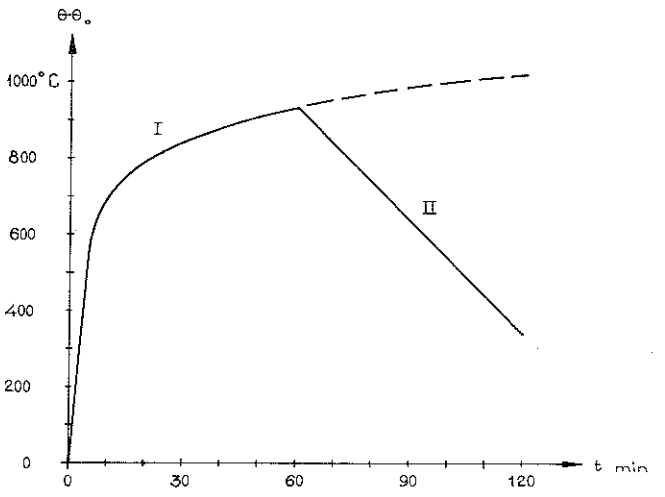

Fig. 4. Swiss standard temperature-time curve relating to fires in enclosed spaces. Curve branch I: Period of temperature rise. Curve branch II: Period of temperature fall corresponding to a linear rate of decrease in temperature of 10° C per min [8].

or – as in the present Swiss standard specifications – in conformity with a sloping rectilinear temperature-time curve, see Fig. 4.

It is seen from these graphs that the standard temperature-time curves used in various countries differ but slightly within the time range 0 to 2 hours, which is of interest in ordinary fires under practical conditions. If the duration of the fire exceeds this value, then the range of variation in the temperature-time curves becomes wider, and hence more manifest. For the set of temperature-time curves reproduced in Fig. 2, the width of this range amounts to 41, 67, 123, and 181° C when the duration of the fire is $t=3$, 4, 6, and 8 hours, respectively. The scatter is found to be remarkably great in the curves shown in Fig. 3, which represent the relation between the duration of a fire and the fire load. In this graph, Curves 1, 2, and 3 refer to the standard relations used in Sweden, in the United States, and in the United Kingdom, respectively, whereas Curve 4 was taken from a Swiss draft standard [8], which is based on results obtained from wood fire tests in compartments with square floor surfaces. For a fire load of 200 kg of wood per m² of floor area, the respective values of the duration of the corresponding fire obtained from these four curves are 4, 4.8, 3.2, and 1.4 hours. This variation illustrates in a striking manner the great differences which exist now at an international level in respect of one of the principal assumptions serving as a basis for estimating and grading structures or structural parts from a fire engineering point of view.

To characterise the process of fire development in such a way as it is done at present in all regulations and recommendations, that is to say, by specifying only a temperature-time curve and a relation between the duration of the fire and the fire load, is a description which is far too stereotyped and incomplete to be regarded as something more than a temporary expedient.

The temperature-time relation which represents the development of a fire in an enclosed room is essentially dependent not only on the amount of combustible materials present in the room, but also on many other parameters. The most important of these parameters are enumerated in what follows.

(1) Position of the fuel in the enclosed room.

(2) Type of fuel.

(3) Dispersion factor (hydraulic radius) and particle shape of the fuel.

(4) Amount of air per unit time supplied to the enclosed room.

(5) Temperature, pressure, and relative humidity of the air supplied to the enclosed room.

(6) Horizontal and vertical co-ordinates of the enclosed room.

(7) Thermal inertia and thermal conductivity characteristics of the structures which bound the enclosed room or are contained in this room.

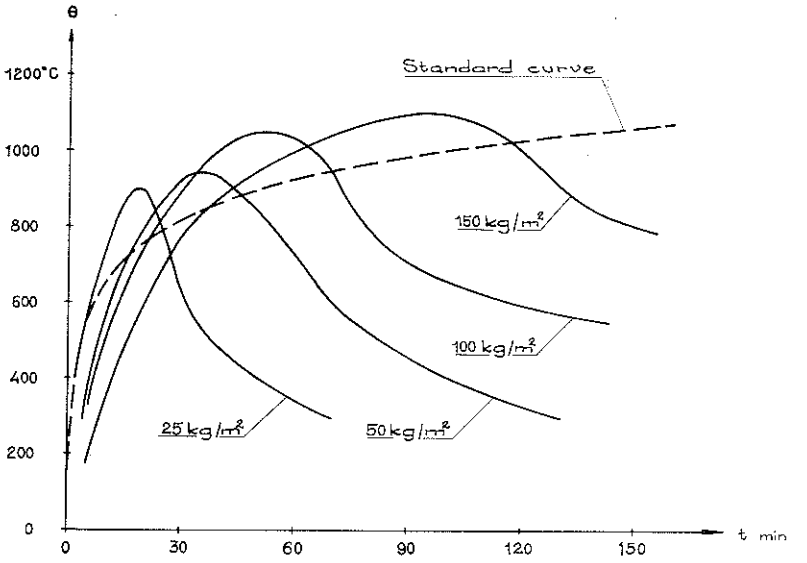

Fig. 5. Temperature-time curves determined by *Mourachev* at fire loads of 25, 50, 100, and 150 kg of wood per m² of floor area, compared with the ISO/TC 92, INSTA 28/2, or DIN 4102—62 standard curve [9].

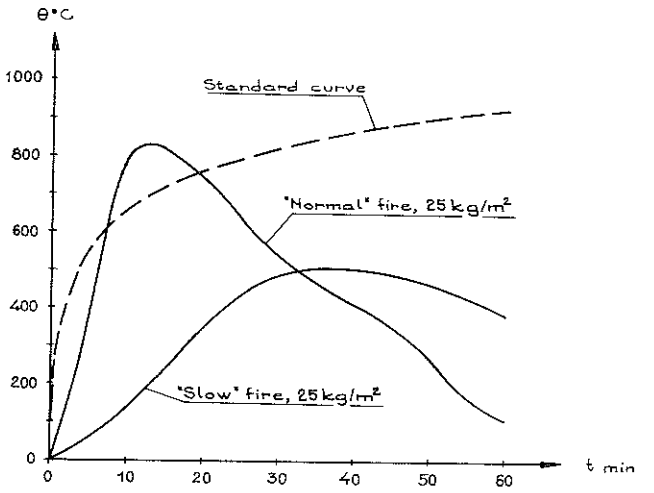

Fig. 6. Temperature-time curves corresponding to "normal" and "slow" combustion, respectively. These curves were determined from fire tests in an enclosed room, where the amount of fuel was 25 kg of wood per m² of floor area [10]. Cf. the ISO/TC 92, INSTA 28/2, or DIN 4102—62 standard curve.

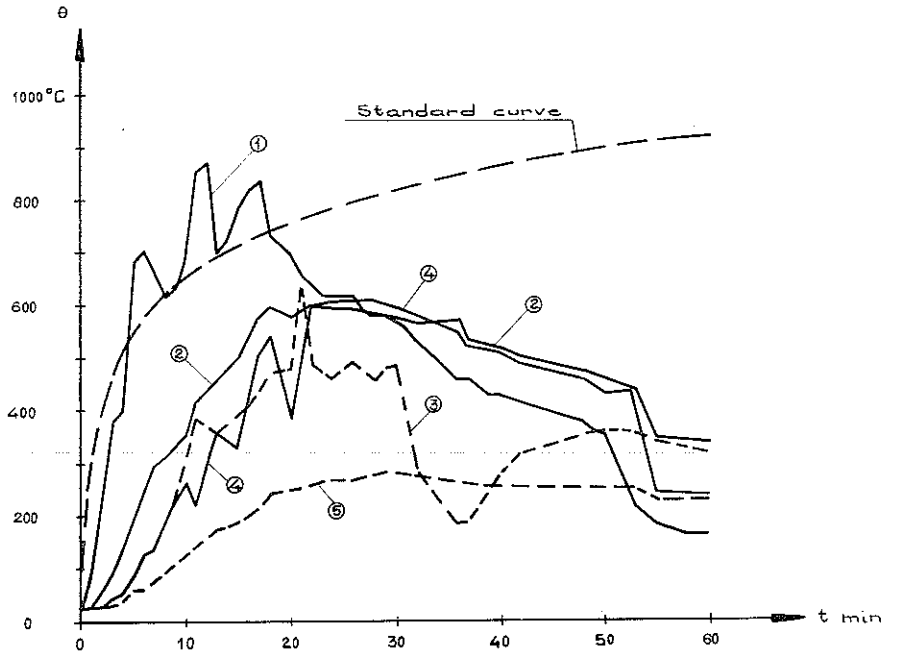

Fig. 7. Temperature-time curves determined from fire tests at a fire load of 25 kg of wood per m^2 of floor area in an enclosed room, $8.7 \times 6.6 \times 3.8$ m^3 in internal dimensions, which contained two symmetrically placed steel frames. One of them was of a light, unprotected type, while the other was protected by concrete [10].

Curve 1: Temperature of the fire at a point situated 65 cm below the centre of the ceiling.
Curve 2: Temperature on the upper surface of the bottom flange at the mid-section of the horizontal member. Light, unprotected steel frame.
Curve 3: Ditto. Heavy, protected steel frame.
Curve 4: Temperature on the inner side of the inner flange at a vertical member section situated 130 cm above the floor. Light, unprotected steel frame.
Curve 5: Ditto. Heavy, protected steel frame.
Cf. the ISO/TC 92, INSTA 28/2, or DIN 4102—62 standard curve.

Fragmentary illustrations of the effects produced by some of these parameters on temperature-time curves will be found in Figs. 5, 6, and 7. In Fig. 5, the curves determined by *Mourachev* [9] from wood fire tests show the effect of variations in the amount of fuel under "normal" conditions of combustion. As regards the above-mentioned relation between the duration of a fire and the fire load, the results given in Fig. 5 can serve to corroborate the Swiss draft standard curve reproduced in Fig. 3. The effect of variations in the quantity of air supplied to the enclosed space per unit time is illustrated in Fig. 6. This graph shows the temperature-time curves which have been

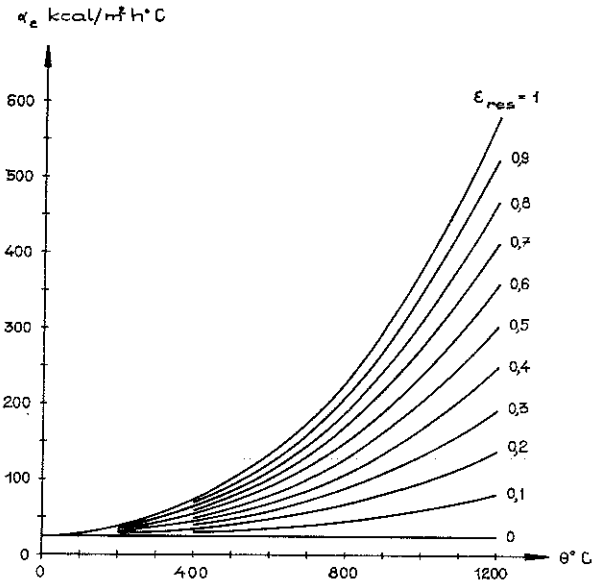

Fig. 8. Calculated theoretical relation between the coefficient of heat transmission, α_e, at the fire-exposed surface of a structural part and the temperature in the enclosed room, θ, for varying values of the resultant emissivity, ε_{res}, which is determined by the relation

$$\frac{1}{\varepsilon_{res}} = \frac{1}{\varepsilon_{fl}} + \frac{1}{\varepsilon_y} - 1$$

where ε_{fl} is the emissivity of the flames and ε_y is the emissivity of the fire-exposed surface of the structural part.

obtained from Swiss fire tests [10] under conditions of "normal" and "slow" combustion when the amount of fuel was 25 kg of wood per m² or floor area. Furthermore, the effects of another two of the above-mentioned parameters influencing the process of fire development, viz., the vertical co-ordinates of the enclosed space and the thermal inertia characteristics of a structure contained in the enclosed space, are illustrated in Fig. 7 [4]. This graph reproduces the temperature-time curves which have been recorded at several points of a compartment in a fire test where the amount of fuel was 25 kg of wood per m² of floor area. These curves relate to an enclosed room, $8.7 \times 6.6 \times 3.8$ m³ in internal dimensions, which contained two symmetrically placed frame structures during the fire test. One of these structures was a light, non-covered steel frame, while the other was a heavy steel frame filled with concrete between the flanges of the structural shapes. Fig. 7 shows that the temperature in the enclosed room increased in a vertical direction from a lower to a higher level. Moreover, it is seen from this graph that the temperatures at the various

points of the light, non-covered steel frame were higher than those at the corresponding points of the heavier, concrete-covered steel frame, which had a greater thermal inertia.

An accurate description of the temperature-time curve representing the process of fire development in an enclosed room is not sufficient as an external characteristic for determining the temperature fields in a structure or a structural part exposed to a fire. In addition, another essential factor which is decisive in this connection is the coefficient of heat transmission through the boundary air layer at the exterior surfaces bounding the structure exposed to the fire. This coefficient is primarily influenced by the convection and radiation conditions. The markedly predominant component of heat transmission is usually that which is due to radiation. In general, this component increases with increase in the temperature of the enclosed room as well as with increase in the resultant emissivity of the fire-exposed surface of the structural part and of the flames or smoulders in the burning zone, cf. Fig. 8 in this respect. This

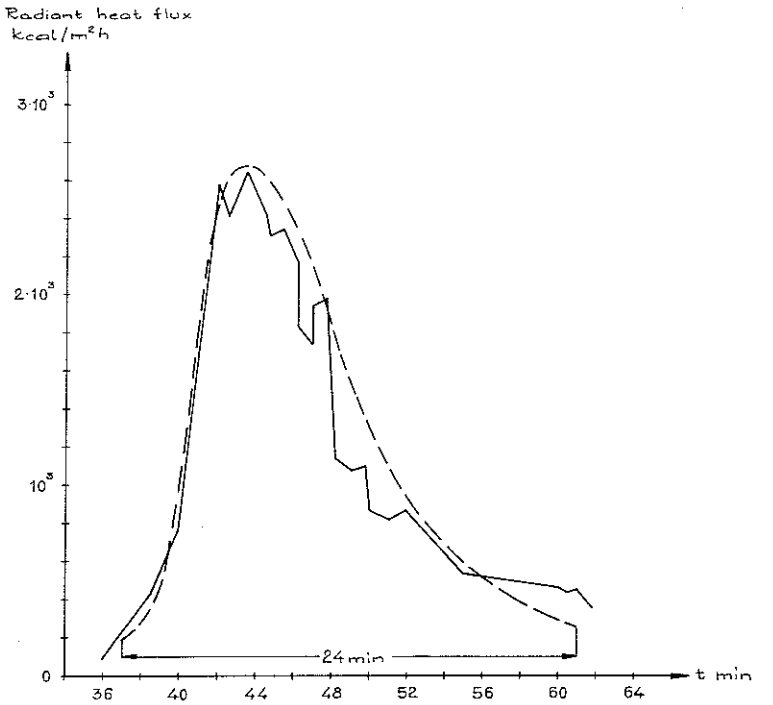

Fig. 9. Variation in the radiant heat flux from a burning timber house with the time. This graph relates to timber house fires at high fire loads. Dash-line curve: Japanese standard curve. Full-line curve: Curve determined from radiation measurements in full-scale tests. The radiant heat flux was measured at a point situated at a distance of 30 m from the source of fire [11].

graph shows a theoretically calculated set of curves which represent the relation between the coefficient of heat transmission at the fire-exposed surface of the structural part and the temperature in the enclosed room for varying values of the resultant emissivity, ε_{res}. These curves are based on the assumption that the coefficient of heat transmission by convection is independent of the temperature, and is equal to 25 kcal per m^2 per h per °C, and that the temperature difference in the boundary air layer is constant in the whoel temperature range met with in the enclosed room, and is equal to 125° C.

The fire engineering literature comprises a very small number of investigations dealing with the conditions of heat transmission associated with fire development. As an isolated example taken from one of these investigations, Fig. 9 reproduces a curve which represents the relation between the radiant heat flux at a point situated at a distance of 30 m from a burning two-storey timber house and the time. This curve has been obtained from full-scale tests in Japan [11]. For the sake of comparison, this graph also shows that standard curve of radiant heat flux distribution, Type A-24, which shall be used in accordance with the relevant Japanese regulations for characterising timber house fires at high fire loads. It is seen that the general shape of the radiant heat flux curve obtained from the tests has verified the correctness of the flux-time relation expressed by the standard curve.

To sum up the above remarks on the process of fire development, it may be stated that the ordinary characterisation of this process in the standard specifications, which give only the temperature-time curve for the enclosed space, is much too extreme a simplification of this problem. At the same time, however, it is also to be noted that the available knowledge of the mechanism of fire development and the associated thermal effects on structures and structural parts is far too incomplete to make it possible at the present time to introduce a more differentiated and functionally more correct characterisation of the process of fire development. Consequently, there is a great need for an active intensification of research in this field. This research should aim at an accurate survey of the effects produced by the above-mentioned parameters on all phases of the process of fire development, viz., the phases of ignition, flaming, smouldering, and cooling, see Fig. 10. Among these phases, the smoulder phase and the cooling phase have practically been left out of account in the investigations which have been published up to now. In the future research into the process of fire development, a high priority should be assigned to accurate studies dealing with characteristics of fires of short duration and to a thorough treatment of the heat transfer conditions which a fire occasions in the boundary air layers at the fire-exposed surfaces of buildings or parts of buildings. In this connection, it is of considerable importance, e.g.

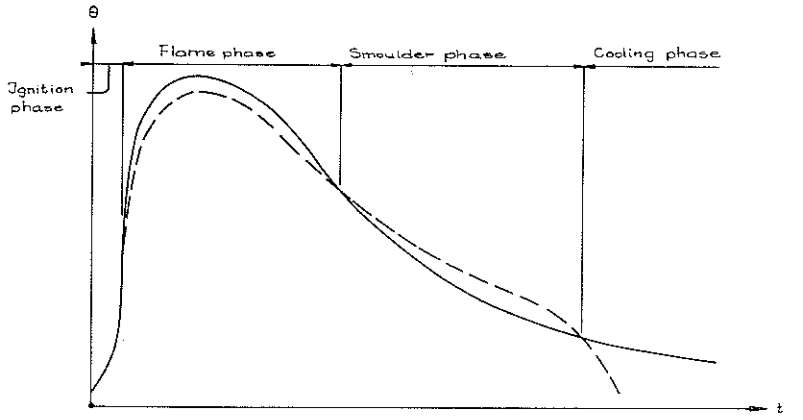

Fig. 10. Main phases of the process of fire development characterised by temperature-time curves of enclosed spaces. Full-line curve: Temperature in the enclosed space determined by means of thermo-couples sheathed in protective tubes. Dash-line curve: Radiation temperature. Cf. e.g. Fig. 15 in [12] and Fig. 12 below.

in the future design and construction of fire testing furnaces, to determine the emissivity of flames, which is subject to wide variations with the type of fuel, etc. For instance, the emissivity of gas flames is about 0.4, while the emissivity of flames in wood fires is comprised within the range from 0.6 to 0.9. Therefore, the structures or structural members subjected to fire tests in gas-fired furnaces are exposed to a radiation effect which is substantially smaller than it is in fires under practical conditions. From a combustion engineering point of view, actual fires may ordinarily be considered to be similar in type to wood fires.

At the present time, there are three main courses open to future fire development research, viz., full-scale tests, model tests, and theoretical calculations dealing with heat balance and mass balance equations.

3.1. **Fire Development Studies Based on Full-Scale Tests**

In fire development studies based on full-scale tests, the most difficult problems are usually encountered in evolving appropriate measurement techniques. Test techniques can also meet with great difficulties in ensuring the idealised testing conditions which are required for isolated studies of the effect of each separate parameter. This is a basic requirement which must be fulfilled in order that the mechanism of fire development may be investigated in detail and in order that the results of such studies may be as generally applicable as possible.

In the Scandinavian countries, relatively extensive studies of the process of fire development are now in progress at the National Danish Institute for Testing Materials (Statsprøveanstalten), Copenhagen, Denmark, and in the Division of Building Construction, Royal Institute of Technology, Stockholm, Sweden. The tests which are being carried out at the National Danish Institute for Testing Materials constitute a part of a research project sponsored by the Liaison Committee of Scandinavian Fire Laboratories (NBS). The object of these tests is to investigate the thermal effects produced by a fire in a single room on the surface layers in a corridor which communicates through an open door with the burning room. The fire development studies conducted at the

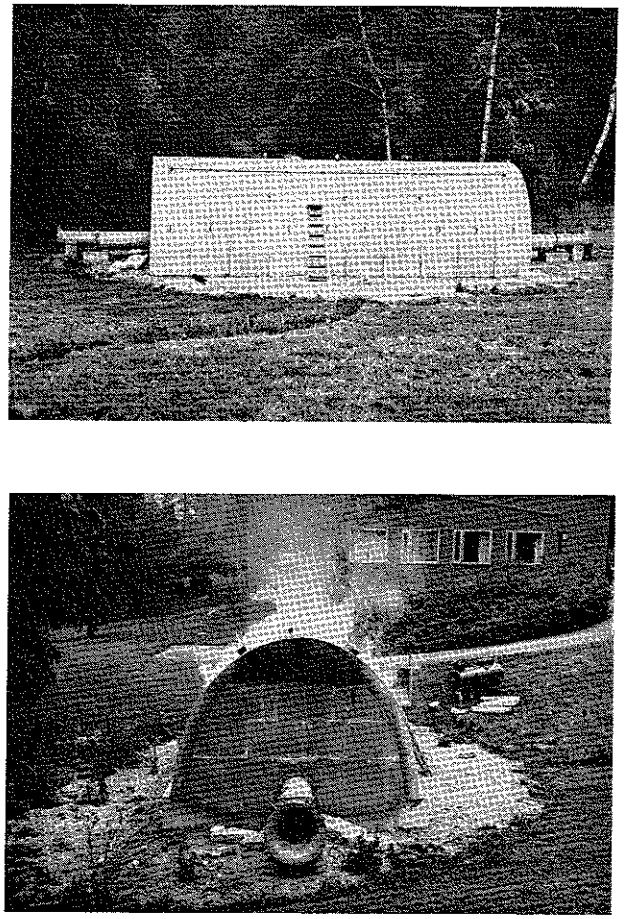

Fig. 11. Test tunnel constructed for fire development studies in the Division of Building Construction, Royal Institute of Technology, Stockholm, Sweden. [12].

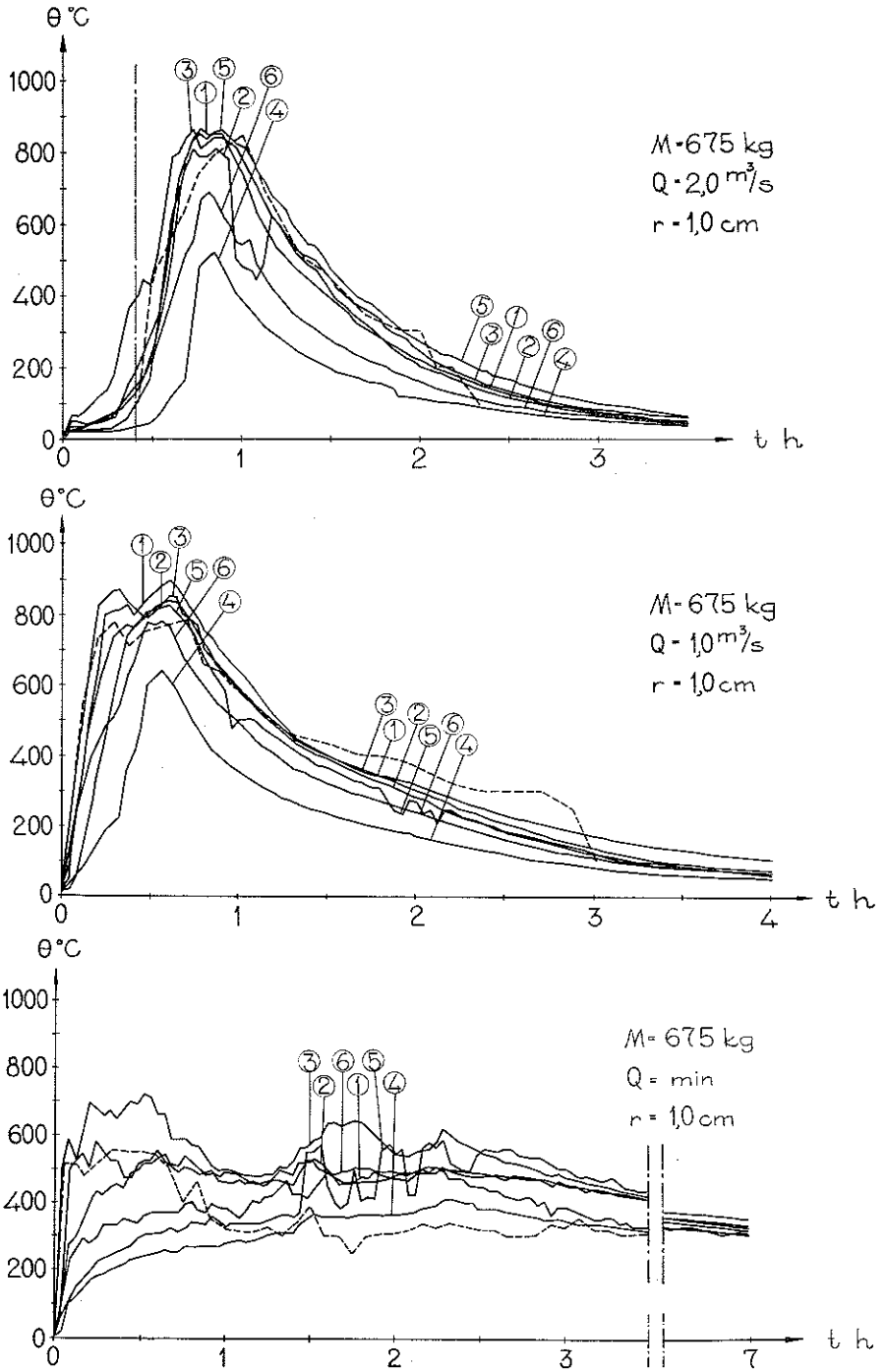

Fig. 12. Temperature-time curves determined in the test tunnel shown in Fig. 11. Fuel: wood. Rates of combustion air supply $Q=2$, 1, and ~ 0 m^3 per sec, respectively. Amount of fuel $M=675$ kg. Hydraulic radius of the fuel $r=1$ cm (1-in. by 4-in. pine boards).

Royal Institute of Technology, Stockholm, are performed in an oblong concrete tunnel of approximately semi-circular cross section, see Fig. 11. The purpose of these tests is to determine accurately, under controlled conditions, the temperature-time curves and the heat transfer conditions in an enclosed space during all phases of the process of fire development. The parameters which are varied in this test series comprise the type of fuel, the amount of fuel, the coefficient of dispersion of the fuel, and the amount of air supplied for combustion to the enclosed space per unit time. The rate of air supply can be regulated and measured by means of a precalibrated fan system. This investigation is being carried out under the direction of *K. Ödeen*. The results which have been obtained up to now are exemplified in Fig. 12 by three sets

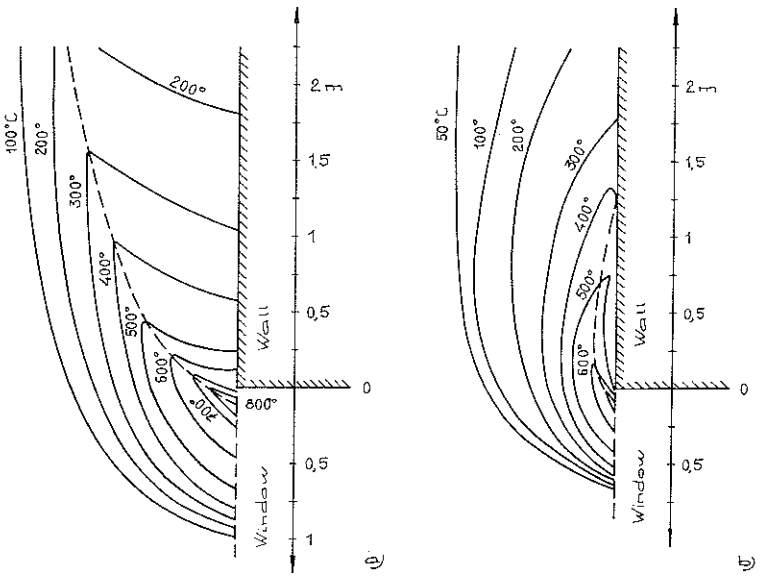

Fig. 13. Isotherms of the air outside an external wall exposed to the flames emerging from a window opening [13]. These isotherms were determined in experimental fires under the conditions stated below.

(a) Concrete building. Fire in a room, 105 m² in floor area and 3.5 m in height to ceiling. Five window openings, 167 cm in height and 91 cm in width each. Amount of fuel: 4400 kg of wood, corresponding to a fire load of 42 kg of wood per m² of floor area, or 12 kg of wood per m² of total surface bounding the room. Window opening factor $A\sqrt{H}/A_t = 0.028\,\mathrm{m}^{1/2}$ where A is the total window area of the room, H is the height of window, and A_t is the total area of the surfaces bounding the room.

(b) Concrete building. Fire in a room, 12.5 m² in floor area and 1.67 m in height to ceiling. One window opening, 100 cm in height and 300 cm in width. Amount of fuel: 500 kg of wood, corresponding to a fire load of 40 kg of wood per m² of floor area, or 10 kg of wood per m² of total surface bounding the room. Window opening factor $A\sqrt{H}/A_t = 0.060\ \mathrm{m}^{1/2}$.

of temperature-time curves, which have been determined in wood fire tests. The respective rates of air supply for combustion were 2, 1, and ~ 0 m^3 per sec. The magnitude of the fire load in all these three tests was 25 kg of wood per m^2 of floor area, or 9 kg of wood per m^2 of total surface bounding the enclosed space. The fuel consisted of 1-in. by 4-in. pine boards, and the hydraulic radius was $r = 1$ cm. The full-line curves in Fig. 12 represent the temperatures which have been measured at various points of the enclosed room by means of thermo-couples sheathed in protective tubes. The corresponding radiation conditions are illustrated by the dash-line curves, which represent the variation in the radiation temperature with the time, and which have been recorded by means of radiation pyrometers.

To exemplify the results of more or less extensive fire development studies based on full-scale tests which have been published in the literature, Fig. 13 shows the temperature fields observed in Japanese investigations [13] in outside air layers adjacent to an external wall which was exposed to flames from a window opening. The knowledge of such temperature fields is essential in estimating the risk of ignition of combustible components entering into an external wall and the risk of external spread of fire from an enclosed room in a storey to enclosed rooms in the storeys situated above. The isotherms reproduced in Fig. 13 were recorded at instants of maximum intensity of the fires whose characteristics are stated in the legend of this graph. It is seen that the fire loads defined in the conventional manner were approximately equal in the two cases under consideration, whereas these cases differed considerably in essential combustion characteristics, primarily, in the window opening factor, $A\sqrt{H}/A_t$. In the test reproduced in Fig. 13 a, the value of this factor was equal to less than half that observed in the test shown in Fig. 13 b. Therefore, it seems to be difficult to draw any detailed conclusions from a comparison between the results obtained from these two tests. However, an important inference can be drawn, namely, that the thermal effect to which an external wall situated above a window opening is exposed when flames emerge from the window opening increases as the ratio of the width to the height of the window opening becomes greater.

3.2. **Fire Development Studies Based on Model Tests**

In order that the results of a model test may be converted into information which is applicable to practical conditions, it is required that the model test shall be carried out so as to satisfy the model laws.

The model laws which govern a complete characterisation of a process of fire development are of an extremely complicated nature, and cannot be regarded as entirely elucidated at the present time. To illustrate the degree of

difficulty of this problem, it may be mentioned that *Faure* [14] has enumerated as many as 9 parameters which determine the convection conditions in the neighbourhood of a source of fire. These parameters are the Reynolds, Schmidt, Prandtl, Mach, and Froude numbers, the first and third Damköhler numbers, as well as two dimensionless quantities. The respective model-scale and full-scale values of these parameters must be equal in order that the results of model tests may be in agreement with the actual conditions in thermal, dynamical, and chemical respects.

If fire development studies are made with a view to limited objectives, then most of the parameters involved in the general case are not required in the application of the model laws. This may be exemplified by a statement of *Thomas* [15], who found that the flames and hot gases which are generated by a fire in the absence of an applied external pressure are ordinarily influenced by forces of only three types, viz., viscous frictional forces, inertial and turbulent frictional forces, and convectional forces, which can be expressed by unique functions of three parameters, viz., the Reynolds, Grashof, and Froude numbers. Then these three parameters determine the ratio of the turbulent frictional force to the viscous frictional force, the ratio of the convectional force to the viscous frictional force, and the ratio of the convectional force to the turbulent frictional force. The respective relations are

$$N_{Re}=\frac{uL}{\nu}$$

$$N_{Gr}=\frac{gL^3}{\nu^2}\left(\frac{\Delta\rho}{\rho}\right)$$

$$N_{Fr}=\frac{u^2}{gL}\left(\frac{\rho}{\Delta\rho}\right) \tag{1}$$

where

u = a characteristic velocity,
L = a characteristic linear dimension,
$\Delta\rho$ = a characteristic relative change in weight (rate of weight ρ loss),
ν = the kinematic viscosity, and
g = the acceleration due to gravity.

Under conditions of predominant turbulence, which characterise the flame stage of a fire, cf. Fig. 10, the viscous frictional forces, and hence also the parameters N_{Re} and N_{Gr} are negligible. Under such conditions, the model laws involved in the process of fire development become extremely simple, and the only requirement to be complied with in such cases is that the value of the

Froude number, N_{Fr}, in a model test shall be equal to that which corresponds to a real full-scale prototype.

If the Froude number is applied as the sole model criterion to the relative flame height, L/D, in a fire, then this flame height will be a function of a single variable, $R^2/g\rho^2D^5$, where R is the rate of burning, ρ is the weight per unit volume (density) of the fuel, and D is a linear dimension that is characteristic of the source of fire [15]. This statement of the problem is illustrated in Fig. 14, which represents the relative height of flames from open fires, where the source of fuel was a crib of wood burning on a square horizontal base, and the value of D was assigned to the side length of the square [16]. The observed values reproduced in this graph were determined during a period of the fire when the rate of burning was approximately constant. The results shown in Fig. 14 were obtained in fire tests carried out by means of cribs of wood, where the side length of the square varied from 6.4 to 152 cm. These results confirm the above-mentioned statement that the characteristics of the flame stage of a fire can to a close approximation be determined by the aid of model tests in which the Froude number, N_{Fr}, serves as the sole decisive model criterion.

For the relative flame height, L/D, we obtain from the observed values given in Fig. 14 the approximate expression

$$\frac{L}{D}=4.4\left(\frac{R^2\cdot 10^6}{D^5}\right)^{0.30} \tag{2}$$

The quantities entering into this relation are expressed in C.G.S. units, that is to say L and D in centimetres, and R in grammes per second. The above

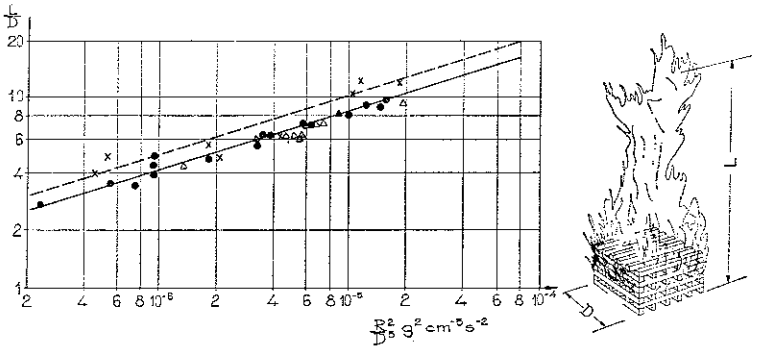

Fig. 14. Relative height of flames, L/D, from open fires. Fuel source: square wooden crib of side length D. Tests made by the Joint Fire Research Organization (●, D=25 to 152 cm), by the U.S. National Bureau of Standards (×, D=6.4 to 91 cm), and by the U.S. Department of Agriculture (Δ, D=15 to 30 cm) [16].

relation has been experimentally verified only in the region from $R^2/D^5 = 2 \cdot 10^{-7}$ to $2 \cdot 10^{-5}$, and shall not be extended to applications lying far outside this region. From the results of similar tests, in which square wood cribs of side length D were burnt in cubical enclosures of edge length D, with *one* vertical side quite open, an expression that is analogous to Eq. (2) can be deduced for the relative height, L/D, of the flames emerging from the enclosure

$$\frac{L}{D} = 4\left(\frac{R^2 \cdot 10^6}{D^5}\right)^{0.33} \tag{3}$$

This relation has been experimentally verified in the range $R^2/D^5 = 4 \cdot 10^{-8}$ to 10^{-6} [15], [16].

To adduce further examples of flame stage characteristics determined by means of model tests, Figs. 15 and 16 show the respective results obtained by *Gross* [17] and by *Simms* and *Hinkley* [15] from studies dealing with the rate of burning of wood fuel.

Fig. 15 relates to the burning of an open square cross pile of wood, which had a side length of 10 b, where b is the width of each individual wood stick. This graph represents the experimentally determined relation between the rate of burning, R, in per cent per sec, and a porosity factor, Φ, which is characteristic of the wood pile, and which is defined by the relation

$$\Phi = N^{0.5} \cdot b^{1.1} \cdot A_v/A_s \tag{4}$$

where

$$A_s = 2nb^2[N(21-n)+n] \tag{5}$$

$$A_v = b^2(10-n)^2 \tag{6}$$

In the above equations, n is the number of sticks per layer, N is the number of layers in the wood pile, A_s is the initial surface area of all sticks entering into the pile exposed to the air, and A_v is the initial open vent surface area of vertical shafts through the pile. The majority of the points plotted in Fig. 15 were determined in the tests where the sticks were made of Douglas fir (Pseudotsuga menziesii). In evaluating the test results, the rates of burning observed in tests on other woods (ash, balsa, and mahogany) were corrected by multiplying them by a factor F, which is equal to the ratio of the thermal diffusivity of Douglas fir to that of the wood under test. In Fig. 15, the rate of burning is scaled, that is to say, represented in the modified form $FRb^{1.6}$, so as to take into account the model scale. As is seen from this graph, the scaled rate of burning, expressed as a function of the porosity factor, Φ, of the wood pile, passes through three distinctly separate stages, which are characterised in what follows.

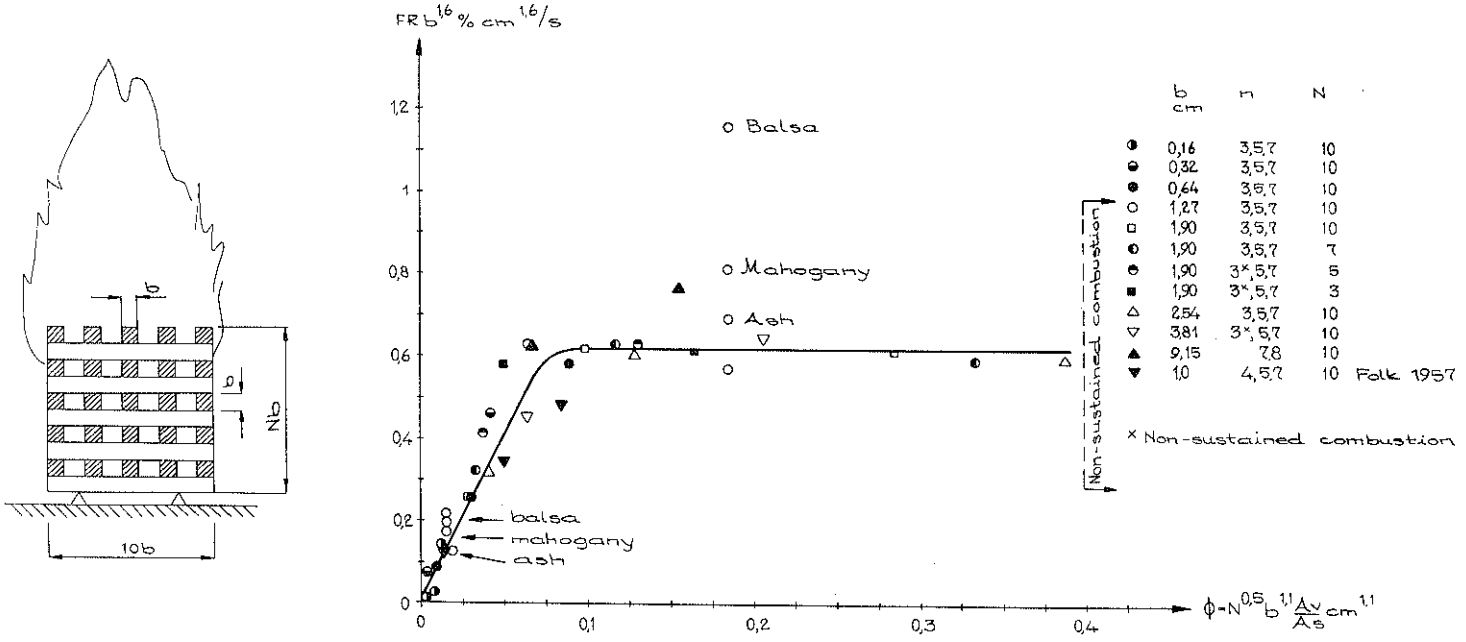

Fig. 15. Relation between the scaled rate of burning, $FRb^{1,6}$, and the porosity factor, ϕ, of the pile of wood. This relation was determined in fire tests made on square cross piles of wood in large, closed rooms [17].

(a) Incomplete combustion, in which the relation between the scaled rate of burning and the porosity factor is approximately linear.

(b) Free combustion, in which the scaled rate of burning is independent of the porosity factor.

(c) Non-sustained combustion; in which the extreme openness of the pile prevents the maintenance of combustion; this is the case when the values of the porosity factor are greater than about $0.4\ cm^{1.1}$.

Fig. 16 shows the relation between the rate of burning, R, and the volume of combustion air supplied per unit time, Q, which has been determined by *Simms* and *Hinkley* in small-scale tests where a square crib was burnt in an enclosure provided with an air intake and an opening in the roof. The values of R represented in this graph relate to that stage of the fire during which the rate of burning was approximately constant. It is seen from Fig. 16 that the rate of burning, R, varied in a marked manner with the volume of combustion air supplied per unit time, Q, at small values of Q. As the rate of air supply became higher, the increase in the rate of burning diminished, and at high values of Q the rate of burning reached an approximately constant value, which corresponds to free combustion, cf. Fig. 15, stages (a) and (b). The tests made by *Webster* and *Raftery* [18] have demonstrated that the magnitude of this upper limiting value of the rate of burning increases to a close approximation linearly with the total amount of fuel in the enclosure. As has been shown by the tests carried out by *Kawagoe* [19], by *Hird* and *Wright* [20], by *Ashton* and *Malhotra* [21], and others, in the region of low values of Q, the rate of burning in an enclosed room provided with a window opening can be represented by the approximate relation

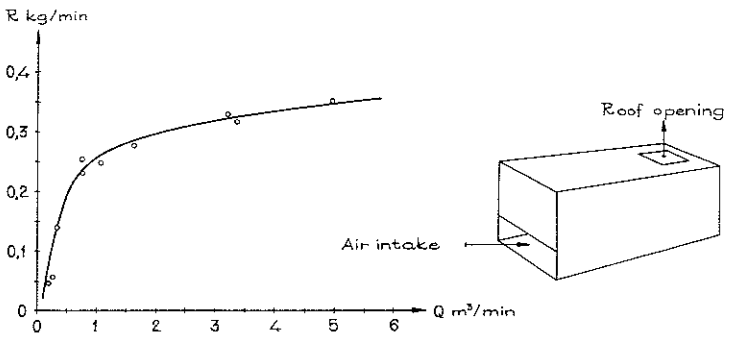

Fig. 16. Relation between the rate of burning, R, and the volume of combustion air supplied per unit time, Q. This relation was determined from small-scale fire tests on a square wooden crib burning in an enclosure. The crib consisted of 6 layers of 6 sticks each, 1 in. by 1 in. by 12 in size. Total weight of crib 2.7 kg [15].

$$R = 6A\sqrt{H} \text{ kg/min} \tag{7}$$

where A is the surface area of the window opening, in square metres, and H is the height of the window opening, in metres. This relation has been verified experimentally for enclosed spaces ranging in volume from 0.2 to 300 m³.

The examples cited in the above indicate the possibilities of determining the characteristics of the flame stage of a process of fire development by means of model tests. As has previously been pointed out, the model laws which govern this stage of the process of fire development are considerably simplified because the stage is usually characterised by greatly predominant turbulence, with the result that the viscous frictional forces, and hence also the associated parameters, i.e. the Reynolds and Grashof numbers, N_{Re} and N_{Gr}, may be disregarded. In the other principal phases of the process of fire development, cf. Fig. 10, the model laws are of a more complicated nature than in the flame stage. All the same, a few test results relating to the ignition stage have been published in the literature, and they indicate that model tests might also be a practicable method of determining the characteristics of this stage [22]. However, our knowledge of this subject is at present too incomplete to justify more definite statements. Finally, as regards the remaining two phases of the process of fire development. i.e. the smoulder stage and the cooling stage, it is only to be pointed out that the literature does not contain any information as to the possibilities of studying these stages by the aid of model tests.

3.3. **Fire Development Studies Based on Theoretical Calculations**

So far as is known to the Author, fire development studies based on theoretical calculations dealing with the heat balance and mass balance equations of the problem under consideration have until quite recently been a field of research that was not represented in the fire engineering literature. The first papers in this field have been published in the first half-year of 1963 by *Kawagoe* and *Sekine* [3] and by *Ödeen* [2]. In these two papers, which have been written independent of each other, the authors have deduced the heat balance equation of fires in enclosed spaces, and, by solving this equation in some basic cases, have calculated the temperature-time curves for enclosed spaces. In both these papers, the problem under study has been dealt with on the simplified assumptions that the temperature in the whole enclosed room is uniform at any moment, that the coefficients of heat transfer at the internal surfaces bounding the room are equal at all points, that the heat flow through the wall, floor, and ceiling or roof structures enclosing the room is one-dimen-

sional, and that this heat flow is uniformly distributed, abstracting from window and door openings, if any.

Kawagoe's and *Sekine*'s paper containes calculated temperature-time curves in the case of an unlimited amount of fuel burning at a constant rate of combustion, R, which is determined by the surface area of the window opening, A, and by the height of the window opening, H, in conformity with the relation, cf. Eq. (7),

$$R = 5.5\, A\sqrt{H} \text{ kg per min} \tag{8}$$

where A is expressed in square metres and H in metres. The effect of the radiant heat flow through the window opening is included in the treatment. The thermal properties of the gaseous products of combustion, as well as those of the materials used for the wall, floor, and ceiling or roof structures, are assumed to be approximately independent of the temperature, and the effect produced

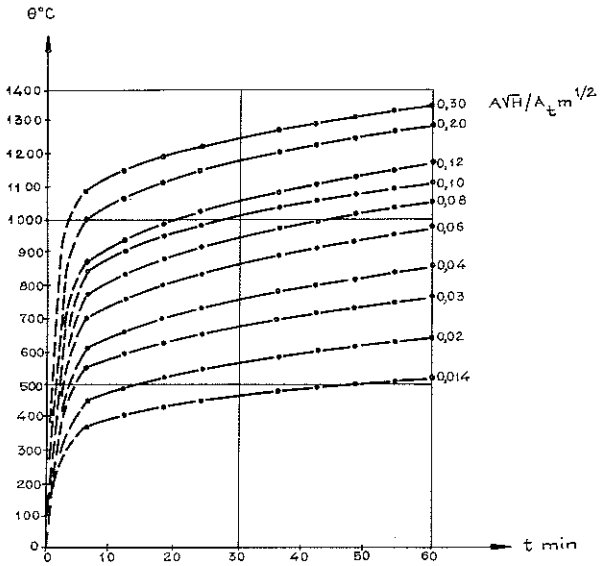

Fig. 17. Temperature-time curves calculated by *Kawagoe* and *Sekine* [3] for combustion of wood fuel burning in a room enclosed by concrete structures and provided with a rectangular window opening of area A and height H. The total area of the surfaces bounding the room is denoted by A_t.
Characteristics: Emissivity of the flames, $\varepsilon_{fl}=1$. Emissivity of the walls, $\varepsilon_y=0.7$. Thermal conductivity of the walls, $\lambda=1$ kcal per m per h per °C. Thermal diffusivity of the walls, $a=0.002$ m² per h. Specific heat of the gaseous products of combustion, $c_{cg}=0.32$ kcal per m³ n.t.p. per °C. Volume of the gaseous products of combustion, $G=4.9$ m³ n.t.p. per kg of wood. Calorific value of the wood fuel, $q=2575$ kcal per kg (corresponding to about 60 per cent combustion).

by the dissociation of the gaseous products of combustion is disregarded. The results published in the paper under review are exemplified in Fig. 17, which shows the calculated temperature-time curves of enclosed rooms with concrete wall, floor, and ceiling or roof structures for several values of the window opening factor, $A\sqrt{H}/A_t$, where A_t denotes the total area of the surfaces bounding the enclosed room, including the window opening. The effect of variations in the thermal properties of the structures enclosing the room is illustrated in this paper by temperature-time curves calculated for three values of the coefficient of thermal conductivity, viz., $\lambda=1$, 0.5, and 0.1 kcal per m per h per °C. On the other hand, the thermal diffusivity, a, was assumed to be constant in all these three cases, and to be equal to 0.002 m² per h.

The paper by *Ödeen* is more general and comprehensive in scope. The basic relations are deduced so as to take into account the effect of the dissociation of the gaseous products of combustion, which is an essential factor at temperatures higher than about 1500° C. Furthermore, these relations take account

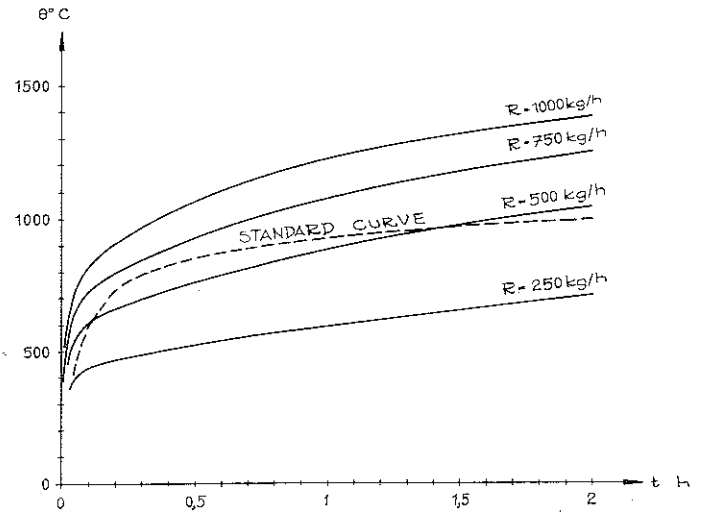

Fig. 18. Temperature-time curves calculated by *Ödeen* [2] for different rates of burning, R. Wood fires burning in a room enclosed by concrete structures, 20 cm in thickness. Characteristics: Volume of the room, $V=46$ m³. Total area of the surfaces bounding the room, $A_t=75$ m². Emissivity of the flames, $\varepsilon_{fl}=0.7$. Emissivity of the walls, $\varepsilon_y=0.9$. Thermal conductivity of the walls, $\lambda=1.3$ kcal per m per h per °C. Thermal diffusivity of the walls, $a=0.0025$ m² per h. Specific heat of the gaseous products of combustion varying with the temperature and taking into account the effect of dissociation, c_{cg}. Volume of the gaseous products of combustion, $G=5.14$ m³ n.t.p. per kg of wood. Calorific value of the wood fuel, $q=4120$ kcal per kg (corresponding to complete combustion of wood having a moisture content of 10 per cent by weight).

of the fact that the thermal properties of the gaseous products of combustion and those of the materials which enter into the structures enclosing the room are dependent on the temperature. However, so far as the thermal properties of the structural materials used for walls, floors, and ceilings or roofs are concerned, their dependence on the temperature is taken into consideration in solving the basic equations, but this is confined to an approximate treatment, which is based on those average values of the thermal conductivity, λ, and the thermal diffusivity, a, which are representative of the temperature range under consideration. This paper contains extensive data in the form of temperature-time curves calculated by means of an electronic computer, which relate to the case where the amount of combustible material (wood fuel) in the enclosed space is unlimited. These curves represent the effects produced by variations in the rate of burning, in the thermal properties of the enclosing and enclosed structures, and in the emissivities of the internal surfaces of the enclosing structures. Moreover, *Ödeen*'s paper presents calculated temperature-time curves which relate to the case where the amount of fuel in the enclosed space is limited. These curves illustrate primarily the effects of changes in the volume of the enclosed space as well as in the magnitude of the rate of burning and in the type of its variation with the time. The results reported in this paper are exemplified in Figs. 18 and 19. The calculated temperature-time curves reproduced in Fig. 18 relate to rooms enclosed by concrete structures, 20 cm in thickness, and correspond to four rates of burning which are constant in time, viz., 250, 500, 750, and 1000 kg of wood per h. The calculated temperature-time curves shown in Figs. 19 a and 19 b refer to rooms enclosed by structures whose thermal properties are representative of concrete and mineral wool, respectively, and correspond to a rate of burning of 500 kg of wood per h. These curves were computed on the assumption that the room contained a concrete structure which varied in volume. As is seen from these graphs, the temperature-time curve is greatly dependent on the rate of burning, on the thermal properties of the enclosing structures, and – primarily when the room is enclosed by structures which are highly heat-insulating and light in weight – on the structures or structural parts contained in the room. Since the variations in a temperature-time curve are of such a high order of magnitude, this is a serious reason for calling in question the correctness of the standard fire testing procedure used at the present time, which is based on a fixed unique temperature-time curve as one of its main principles. An obvious improvement of this procedure would be to replace this stipulation concerning a fixed temperature-time curve by a requirement which specifies a fixed curve representing the combustion energy supplied per unit time to the fire testing furnace as a function of the time.

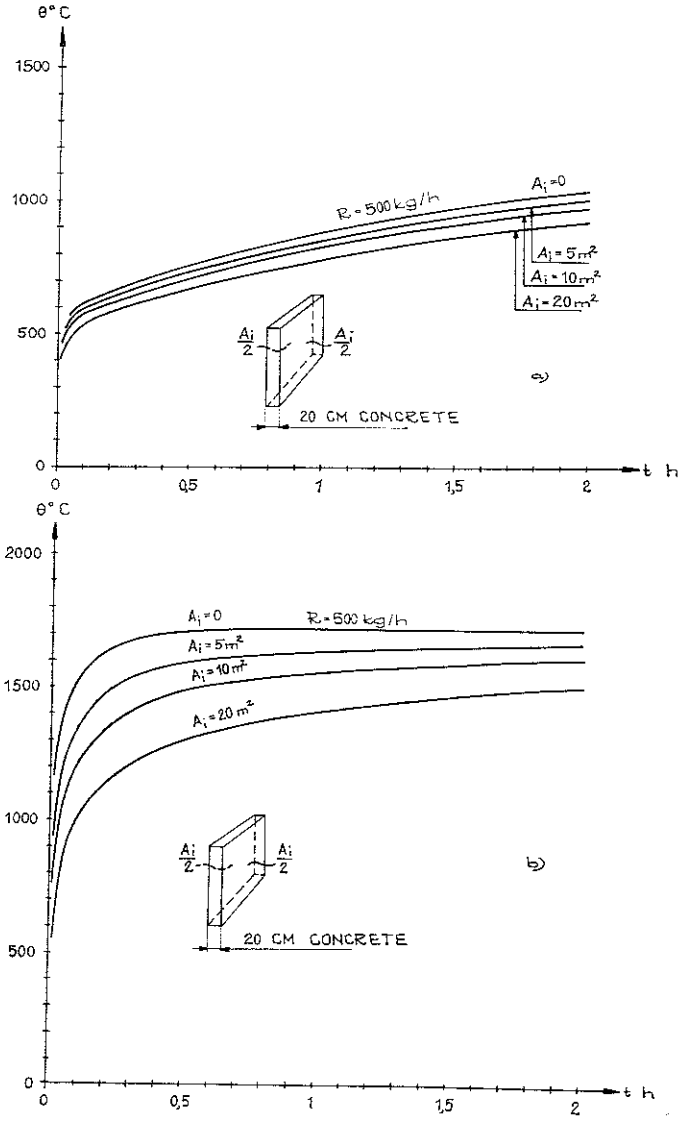

Fig. 19 a and Fig. 19 b. Temperature-time curves calculated by *Ödeen* [2] for a rate of burning of 500 kg per h. Wood fires burning in a room which contains a concrete wall, 20 cm in thickness, and which is enclosed by structures made of concrete, 20 cm in thickness (Fig. 19 a) or mineral wool, 20 cm in thickness (Fig. 19 b).
Characteristics: In Fig. 19 a, the same as in Fig. 18. In Fig. 19 b, thermal conductivity of the walls, $\lambda = 0.20$ kcal per m per h per °C, thermal diffusivity of the walls, $a = 0.01$ m² per h; other data as in Fig. 18.

The papers by *Kawagoe* and *Sekine* and by *Ödeen* which have been briefly reviewed in the above have cleared a new basic way of approach to a differentiated, comparatively inexpensive, and relatively rapid determination of the temperature conditions associated with fires in enclosed spaces. It appears natural that the methods of calculation evolved in these two papers should be included as an important stage in a future, more highly developed procedure of fire engineering design devised in accordance with the general principles stated in Chapter 1. For a given fire load, which implies a known calorific value of the fuel, as well as known characteristics concerning the rate of burning and the emissivity, the above-mentioned methods of calculation incorporated in such a design procedure will make it possible to determine in each individual case all phases of the process of fire development, including a realistic temperature-time curve which takes into account the actual dimensions of the enclosed space, the window and door opening conditions as well as the thermal properties of the enclosing and enclosed structures.

4. Thermal Properties of Common Structural Materials in Temperature Range Associated with Fires

For calculating the temperature field due to an external thermal effect produced by a fire on a structure or a structural part, it is required to know two thermal characteristics of the structural materials in question, viz., the thermal conductivity, λ, and the specific heat, c_p. For the materials exposed on the free surfaces of the structure or the structural part, it is moreover necessary to know a third thermal characteristic, namely, the emissivity, ε_y. Alternatively, the characterisation of a material given by the thermal conductivity *and* the specific heat can be replaced by a characterisation in terms of the thermal conductivity *or* the specific heat in combination with the thermal diffusivity, a, which is determined from the relation

$$a=\frac{\lambda}{\gamma c_p} \tag{9}$$

where γ is the weight per unit volume of the material.

A factor which complicates the calculations of temperature fields is the circumstance that the thermal conductivity, λ, as well as the specific heat, c_p, in the normal case, and also the emissivity, ε_y, in special cases, are dependent on the temperature to an extent that cannot be disregarded in calculations.

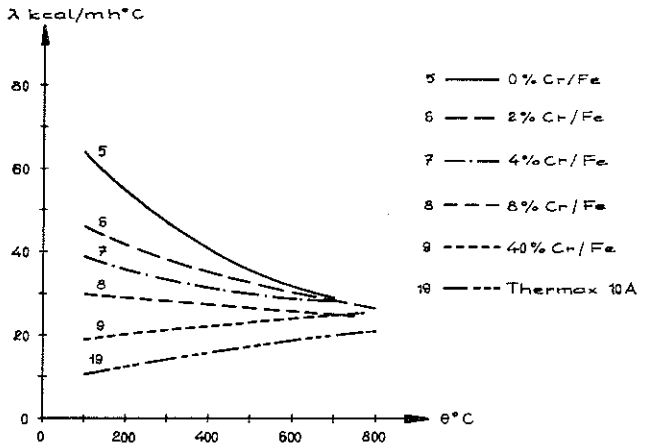

Fig. 20. Variation in the thermal conductivity, λ, with the temperature. Alloy steels varying in chromium content. Thermax 10 A steel is a heat-resistant steel having the following composition, in per cent: Cr 20, Ni 12, Si 2, and C 0.12 [23].

Further complications arise when the material has an initial moisture content, and when the material undergoes changes in internal structure in the course of heating caused by fire.

At the present time, the available information on the above-mentioned characteristics of the structural materials which are used in building construction must unfortunately be described as extremely fragmentary and decidedly insufficient for practical calculations of temperature fields associated with fires. This inadequacy is particularly pronounced when it is required to deal with those changes in the thermal properties which are bound up with structural transformations of the materials. Among the essential problems which, to the Author's knowledge, have so far been left out of consideration in investigations concerning the thermal properties of building materials, there are two that deserve mention in this connection, viz., first, the effects of variations in the rate of heating, and second, the curves representing the thermal conductivity and the specific heat as functions of the temperature during the period of recovery after heating.

In order to illustrate to a limited extent the present scope of information on the thermal properties of building materials, some data on the thermal

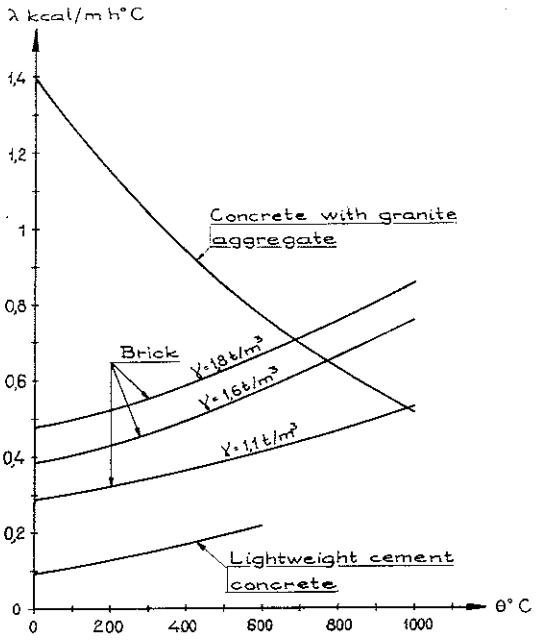

Fig. 21. Variation in the thermal conductivity, λ, with the temperature. Concrete made with granite aggregate, brick, and lightweight cement concrete [2], [24] to [26].

conductivity, λ, the specific heat, c_p, and the thermal diffusivity, a, which have been taken from the literature are reproduced in Figs. 20 to 25.

Figs. 20 and 23 show some characteristics of steels. Fig. 20 represents the relation between the thermal conductivity and the temperature for alloy steels varying in chromium content. Fig. 23 shows the variation in the thermal diffusivity with the temperature for some carbon, low-alloy, and high-alloy grades of steel. It is seen from these graphs, for instance, that the thermal properties are highly sensitive to the carbon and alloy contents of the steel in the lower portion of the temperature range met with in fires. This sensitivity decreases as the temperature increases, and when the temperature exceeds about 800° C, the thermal properties of all the grades of steel included in the above graphs become approximately equal. The thermal characteristics of the ferritic and austenitic steels in the whole temperature range that is of interest in connection with fires are relatively little dependent on the temperature.

The thermal properties of non-metallic building materials are illustrated in Figs. 21, 22, 24, and 25. Among these graphs, Figs. 21 and 22 show the variation in the thermal conductivity with the temperature, and Fig. 24 represents the variation in the specific heat with the temperature. All the curves shown in the last-mentioned three graphs are based on determinations which were made on initially dry materials. The conditions that are characteristic of materials having an initial moisture content are illustrated in Fig. 25. The curves reproduced in this graph relate to gypsum having an initial moisture content of 5 per cent by weight, and were constructed by *Harmathy* [31] on

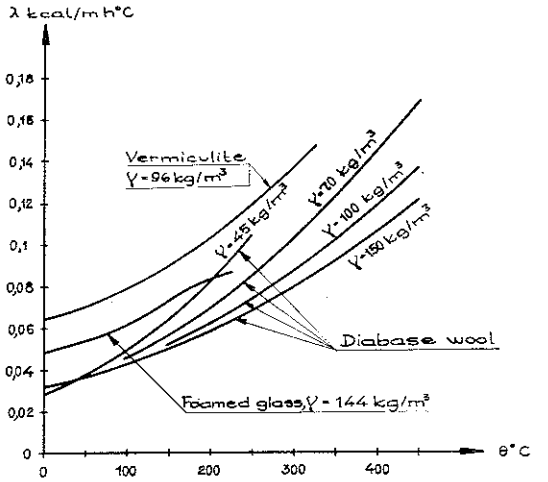

Fig. 22. Variation in the thermal conductivity, λ, with the temperature. Diabase wool, foamed glass, and vermiculite [26]. [28].

the basis of data taken from the literature. These curves, which also include the effect of structural transformations in gypsum, represent the enthalpy per unit volume, I, Fig. 25 a, the specific heat per unit volume, $\bar{c}_p$, Fig. 25 b, determined by the expression

$$\bar{c}_p = \frac{\partial I}{\partial \theta} \tag{10}$$

and the thermal conductivity, λ, Fig. 25 c. The physico-chemical changes which are of importance in this connection at a rising temperature are enumerated in what follows.

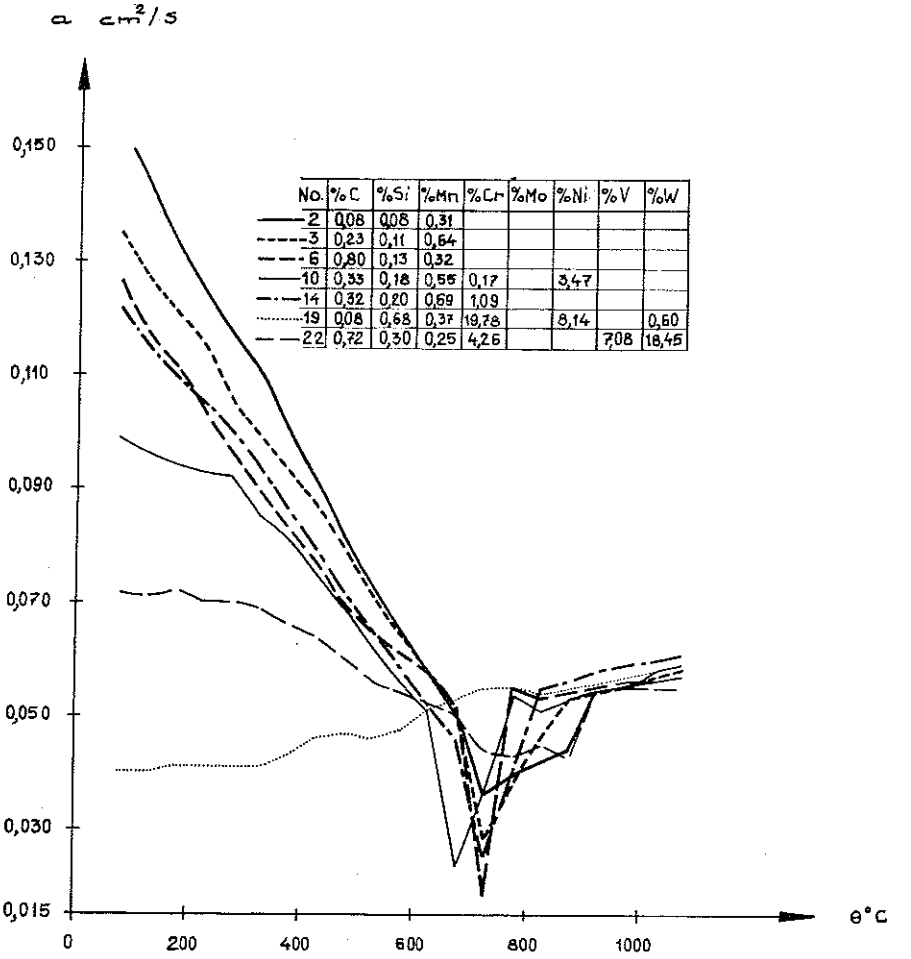

Fig. 23. Variation in the thermal diffusivity, a, with the temperature. Carbon steels, Nos. 2, 3, and 6, low-alloy steels, Nos. 10 and 14, and high-alloy steels, Nos. 19 and 22 [23].

(a) At 100° C, removal of adsorbed water (ds).

(b) At 150 to 220° C, removal of crystal water in two steps (dh).

(c) At 360° C, transformation of soluble $CaSO_4$ into an insoluble modification (tr).

(d) At 1230° C, dissociation of a small part of $CaSO_4$ into CaO and SO_3.

(e) At 1380° C, fusion of the eutectic mixture of CaO and $CaSO_4$.

These curves are applicable on condition that the rate of heating is relatively high. If the rate of heating is comparatively low, then the removal of crystal water takes place at considerably lower temperatures, and in that case the enthalpy curve assumes the form indicated by the dash-line branch in Fig. 25 a.

The available information on the emissivity, ε_y, of building materials in the temperature range associated with fires is at present still more incomplete than that on the thermal conductivity and the specific heat. The variation in the emissivity with the temperature is by no means inconsiderable, as may be

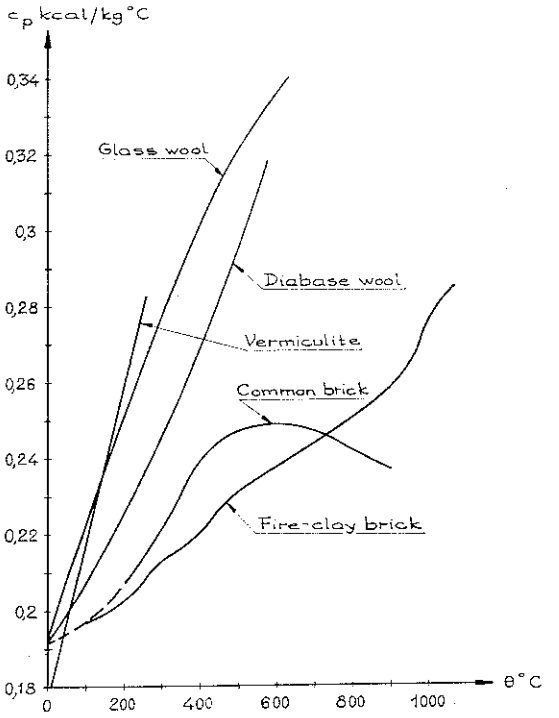

Fig. 24. Variation in the specific heat, c_p, with the temperature. Fire-clay brick, common brick, diabase wool, glass wool, and vermiculite [26], [29], [30].

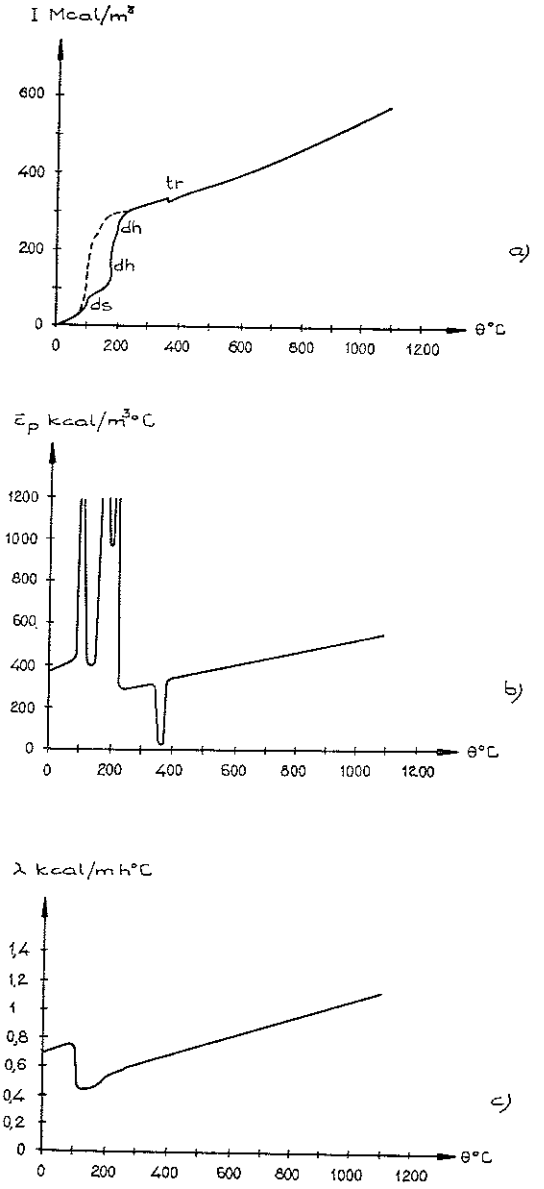

Figs. 25 a, 25 b, and 25 c. Variations in the enthalpy, I, in the specific heat, $\hat{c}_p$, and in the thermal conductivity, λ, with the temperature. Gypsum having a weight per unit volume of 1250 kg per m³ and an initial moisture content of 5 per cent by weight. These curves include the effects of the physico-chemical transformations caused by heating [31] to [35].

Table 2. Variation in emissivity with temperature

Surface	Temperature, θ, °C	Emissivity, ε_{yn}
Aluminium	230 to 580	0.039 to 0.057
Nickel	230 to 380	0.070 to 0.086
Steel	180 to 230	0.052 to 0.064
Zinc	230 to 330	0.045 to 0.053
Lead	130 to 230	0.057 to 0.075

seen from Table 2 [36], where certain temperature intervals are brought into relation with the associated ranges of variation in the emissivity, ε_{yn}, corresponding to radiation from some bright-polished metal surfaces in the direction of the normal to the surface.

5. Strength and Deformation Properties of Common Structural Materials in Temperature Range Associated with Fires

In order that the temperature fields calculated with reference to an external thermal effect produced by a fire on a structure or a structural part may be interpreted in terms of the load-bearing capacity available at different instants throughout the duration of the fire, it is required to possess detailed information which shows how the strength and deformation properties of the structural materials vary with the temperature in the temperature range associated with the fire. At the present time, the scope of information on this subject is relatively wide so far as metallic materials are concerned, but it is on the other hand conspicuously fragmentary as regards such structural materials as ordinary concrete and lightweight concrete.

The strength and deformation properties of a structural material are more or less affected by heating as a consequence of intercrystalline, molecular, or atomic processes. As the temperature rises, the vibrations of the atoms around their points in the space lattice become greater. Structural transformations can occur at definite temperatures, which are characteristic of each material. For example, the mild structural steels, which have carbon contents ranging from about 0.05 to about 0.2 per cent, are characterised by four clearly marked critical points in the interval from ordinary room temperature to +1400° C. In composite materials of the concrete type, the differences in the linear coeffi-

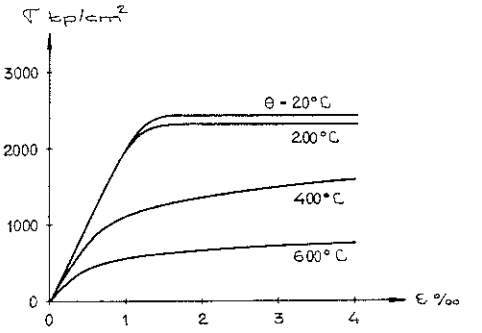

Fig. 26. Stress-strain curves characteristic of mild structural steel under the action of tensile loads in the temperature range from 20 to 600° C. These curves were determined at a standard rate of loading on test specimens kept for about $1\frac{1}{2}$ h before the application of the loads at the respective testing temperatures, which had reached a steady state during a heating period of about 2 h [37].

cient of thermal expansion between the constituent materials, cf. Fig. 33, give rise to internal stresses, which can produce substantial effects on the strength and deformation properties of the composite material by causing crack formation and creep phenomena. These effects can be intensified in a not inconsiderable degree by evaporation of water in the interior of the material subjected to heating, as this causes an increase in internal stresses. A further decrease in the strength and in the deformational rigidity of a material takes place in materials possessing a high thermal inertia, e.g. ordinary concrete and lightweight concrete, because the temperature distributions in these materials are pronouncedly non-uniform, and result in stresses which are set up in structures or structural parts made of such materials, when they are exposed to a fire. On account of these stresses, the strength and deformation properties of these materials determined on test specimens are greatly dependent on several factors, e.g. the shape of the test specimen, the size of the test specimen, the rate of heating, and the duration of the heating period. Since the creep characteristics of materials are manifestly dependent on the temperature, the rate of heating and the duration of the heating period also produce substantial effects on the strength and deformation properties of materials which have a low thermal inertia, and which are therefore rapidly heated all through, e.g. metals.

The strength and deformation properties of the commonly used structural materials at temperatures which are met with in connection with fires are

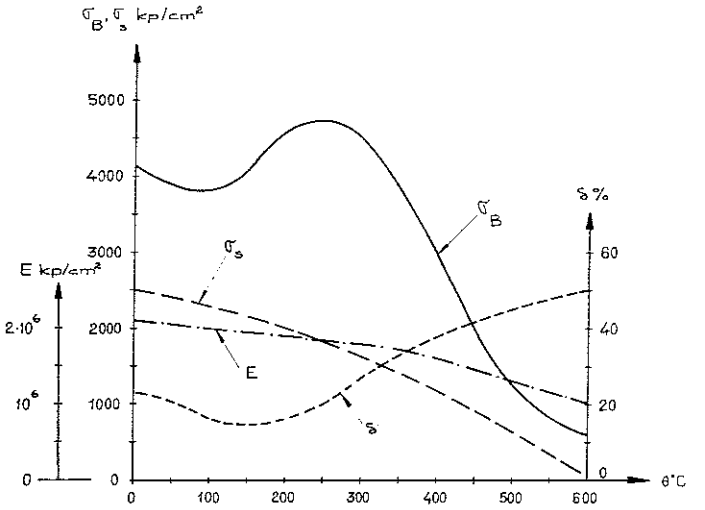

Fig. 27. Variations in the tensile strength, σ_B, in the yield point stress, σ_s, in the modulus of elasticity, E, and in the ultimate elongation, δ, with the temperature. These curves are approximately characteristic of the Swedish standard grade St 37 mild structural steel subjected to short-time tensile loads in a heated state [38].

summarily illustrated in Figs. 26 to 38, which cover steel, aluminium alloys, ordinary concrete, and lightweight concrete.

Figs. 26 to 30 relate to steel. Figs. 26 and 27 refer to *mild structural steels*, while Figs. 28 to 30 deal with the high-tensile steels which are used for prestressed concrete. Fig. 26 [37] shows how the stress-strain diagram of a mild structural steel changes with the temperature, and how the yield point stress region, which is strongly marked at ordinary room temperature, gradually disappears as the temperature becomes higher. Fig. 27 [38], which approximately refers to the Swedish standard steel grade St 37, illustrates the variations in the tensile strength, σ_B, in the yield point stress or – at higher temperatures – in the 0.2 per cent yield strength, σ_s, in the short-time modulus of elasticity, E, and in the ultimate elongation, δ, with the temperature. As is seen from this graph, the increase in the temperature has a favourable effect on the tensile strength, σ_B, when the steel is heated to a temperature up to 300 or 350° C, and then the strength rapidly diminishes as the temperature becomes still higher. It is furthermore seen that the yield point stress or the 0.2 per cent yield strength, σ_s, and the short-time modulus of elasticity, E, decrease continuously as the temperature increases. Moreover, this graph shows that the ultimate elongation, δ, tends to decrease with rise in temperature within the range from 0 to 150° C, and then tends to increase. It is of interest to note, among other things, that the temperature produces on the modulus of elasticity, E, a considerably smaller effect than on the yield point stress, σ_s. As a consequence of this fact, the processes of deformation of load-bearing structures made of mild structural steels, and the failures due to elastic instability of these structures, are less sensitive to the effects of fires than those phenomena of failure which are bound up with a certain definite factor of safety referred to the yield point stress. All the curves reproduced in Figs. 26 and 27 have been obtained from tension tests on specimens which were stabilised at the respective temperatures during relatively short periods of time before they were submitted to the standard tests. An increase in the duration of the heating period causes a reduction in the tensile strength, σ_B, and in the yield point stress, σ_s, as well as a simultaneous increase in the ultimate elongation, δ. This is illustrated in Fig. 30 b, as concerns the yield point stress in the case of a high-tensile, cold-stretched steel used for concrete reinforcement. The effects of heating on the strength and deformation properties of mild structural steels under the action of compressive loads have so far been studied to an extremely small extent, but the results of isolated tests reported in the literature [7] indicate that the yield point stress in compression is somewhat less sensitive to temperature in the range from 350 to 600° C than the yield point stress in tension.

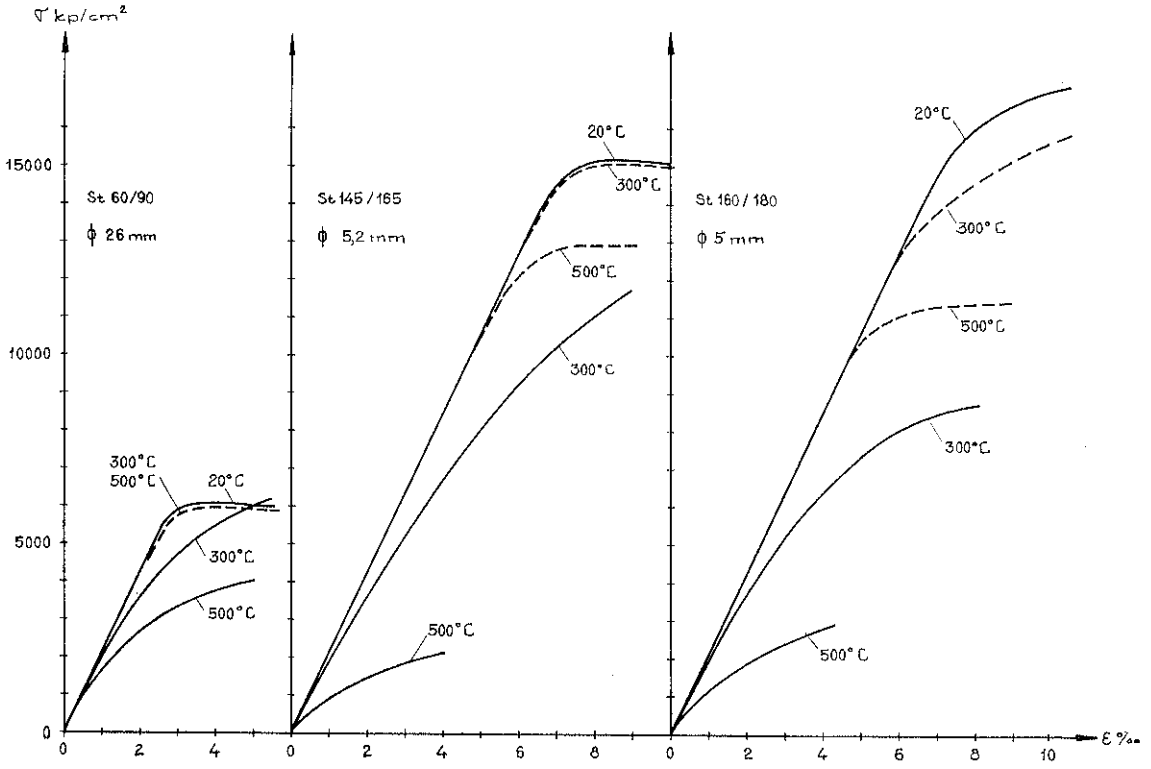

Fig. 28. Stress-strain curves characteristic of three standard steel grades, viz., a hot-rolled steel, St 60/90, a hardened steel, St 145/165, and a cold-drawn steel, St 160/180, subjected to short-time tensile loads in a heated state (full-line curves) or in a cooled-down state efter heating (dash-line curves) [39].

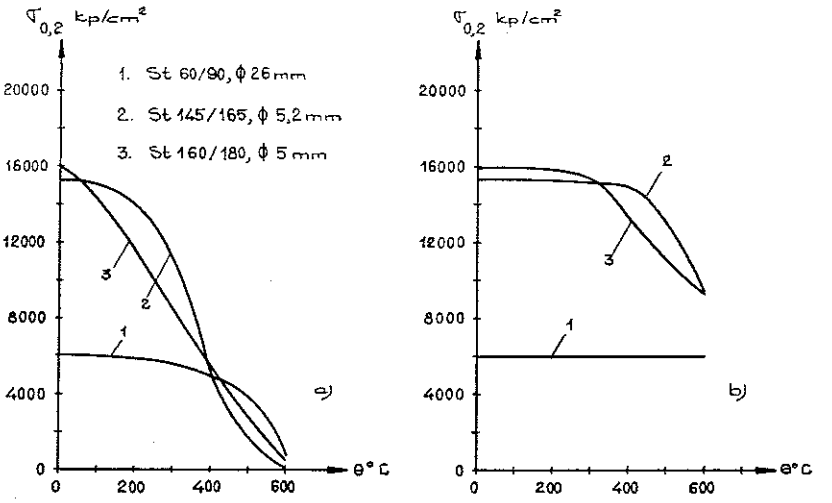

Fig. 29. Variations in the 0.2 per cent yield strength in a heated state (Fig. 29 a) and in the 0.2 per cent residual yield strength (Fig. 29 b) with the heating temperature, θ. These curves were determined in short-time load tests on tensile test specimens made of St 60/90 hot-rolled steel (Curves 1), St 145/165 hardened steel (Curves 2), and St 160/180 cold-drawn steel (Curves 3) [39], [40].

In comparison with the mild, naturally hard structural steels, the high-tensile *prestressing steels* are characterised by strength and deformation properties which are considerably more sensitive to heating. Figs. 28 and 29 [39], [40] illustrate the behaviour of three standard steel grades, viz., a hot-rolled steel, St 60/90, a hardened prestressing steel, St 145/165, and a cold-drawn prestressing steel, St 160/180. Fig. 28 represents the stress-strain diagrams which correspond to temperatures of 20, 300, and 500° C, respectively, and which have been obtained from tests made on specimens in a heated state (full-line curves) or in a cooled-down state after heating (dash-line curves). Fig. 29 shows the variation in the 0.2 per cent yield strength, $\sigma_{0.2}$, and refers to the strength at elevated temperatures (Fig. 29 a) as well as to the residual strength after cooling down (Fig. 29 b). As may be seen from these graphs, the 0.2 per cent yield strength of the naturally hard steel grade St 60/90 at high temperatures does not decrease to half its initial value until the temperature reaches 540° C, whereas the corresponding reduction in the strength of the hardened prestressing steel St 145/165 and the cold-drawn prestressing steel St 160/180 is already reached at temperatures of 370 and 320° C, respectively. When the naturally hard steels were heated in the temperature range from 0 to 600° C, their residual strength was not appreciably reduced in comparison with their initial strength, whereas the residual strength of the hardened and cold-stretched

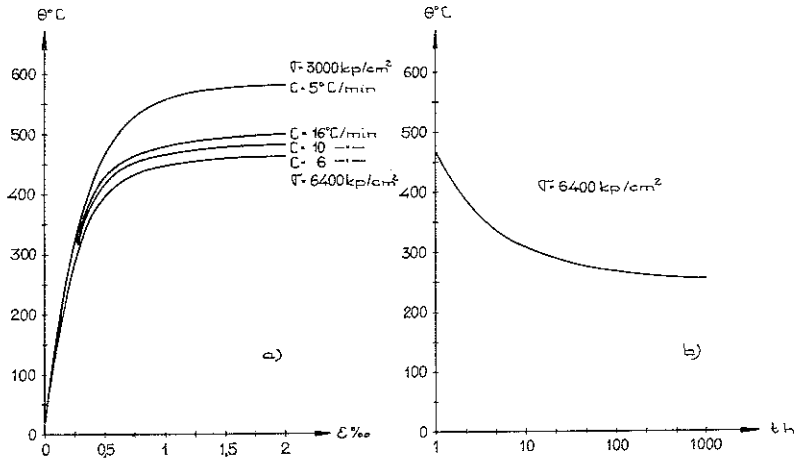

Fig. 30. Relations between the temperature of the steel, θ, and the relative strain, ε, at a varying tensile stress, σ, and a varying rate of heating, c (Fig. 30 a) and between the temperature of the steel, θ, and the time to failure by yielding, t, at a constant tensile stress, $\sigma = 6400$ kp per cm² (Fig. 30 b). These curves were determined in load tests on tensile test specimens made of Swedish standard grade HJS 80/105 cold-stretched prestressing steel [42].

prestressing steels began to diminish to a noticeable degree when the temperatures exceeded about 400° C and about 300° C, respectively.

The stress-strain curves reproduced in Figs. 28 and 29 apply to heating periods of relatively short duration. More extensive investigations dealing with the effects produced by the rate of heating on the strength properties have been made on several grades of prestressing steels by *van Hoogstraten* [41] and on the Swedish standard grade HJS 80/105 cold-stretched prestressing steel by the Halmstads Järnverks AB (Halmstad Ironworks Co., Ltd.), Sweden [42]. Fig. 30 exemplifies the results of the last-mentioned investigation. Fig. 30 a represents the relative strain, ε, as a function of the temperature, θ, of the steel at a tensile stress $\sigma = 3000$ kp per cm² and at a rate of heating $c = 5°$ C per min, as well as at a tensile stress $\sigma = 6400$ kp per cm² and at three rates of heating, viz., $c = 6$, 10, and 16° C per min. Fig. 30 b reproduces the relation between the temperature, θ, of the steel and the time to failure by yielding, t, at the tensile stress, 6400 kp per cm². The curves relating to a tensile stress of 6400 kp per cm² show, among other things, that a decrease in the rate of heating from 16 to 6° C per min reduced the critical temperature of the steel, at which the test specimen subjected to a tensile load failed by yielding, from 500 to 460° C. As is furthermore seen from these curves, when the duration of the heating period at a constant temperature of the steel increased from 1 h to 2, 5, 10, and 100 h, the critical temperature corresponding

to failure by yielding decreased from 470° C to 390, 330, 310, and 270° C, respectively.

The characteristic effects produced on the strength and deformation properties of *aluminium alloys* by temperatures associated with fires are illustrated fragmentarily in Figs. 31 and 32. These graphs relate to a non-heat-treatable (non-hardenable) alloy, AlMg 2.5, and to two heat-treatable alloys having a higher strength, AlMgSi 1 and AlCuMg [43] to [46]. Moreover, the graph representing the variation in the modulus of elasticity, E, with the temperature in Fig. 32 also includes a sintered aluminium powder, SAP. This is a more

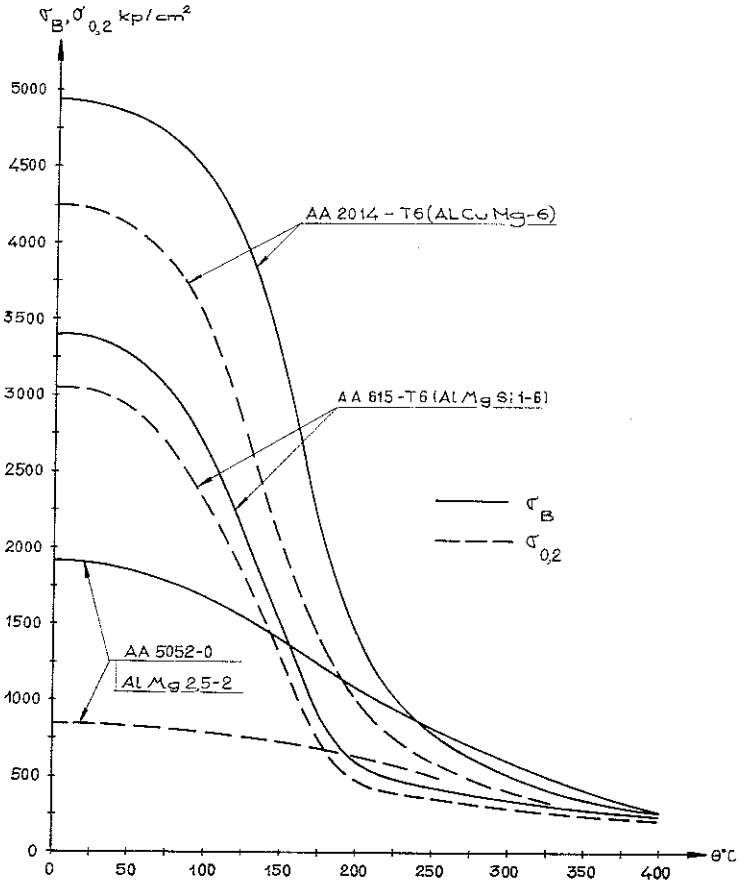

Fig. 31. Variations in the tensile strength in a heated state, σ_B, (full-line curves) and in the 0.2 per cent yield strength in a heated state, $\sigma_{0.2}$, (dash-line curves) with the heating temperature, θ. These curves were determined in short-time load tests on tensile test specimens made of two heat-treatable aluminium alloys, AlCuMg-6 and AlMgSi 1—6, as well as of a non-heat-treatable aluminium alloy, AlMg 2.5—2 [43], [45].

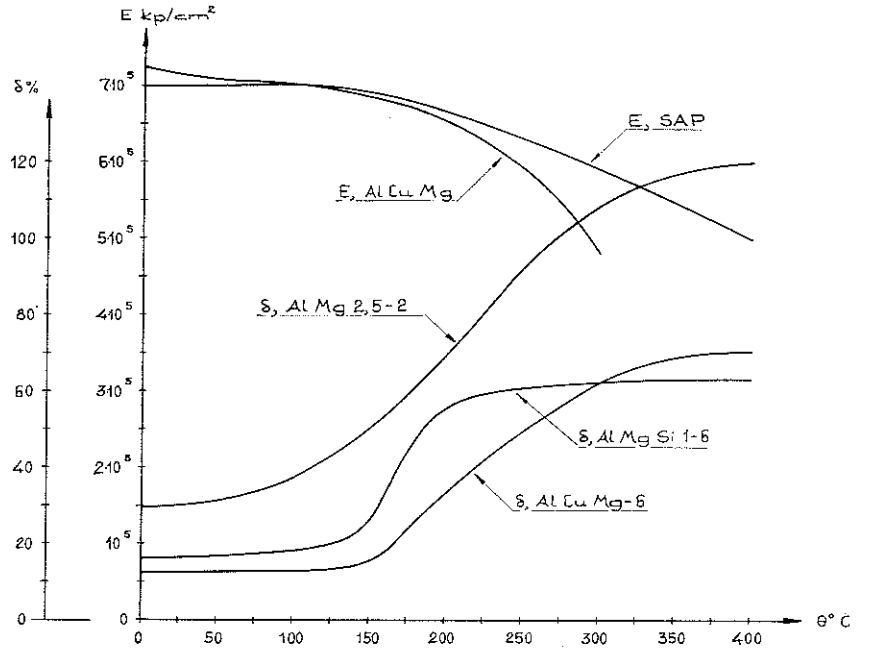

Fig. 32. Variations in the ultimate elongation, δ, and in the modulus of elasticity, E, with the heating temperature, θ. These curves were determined in short-time load tests on tensile test specimens made of three aluminium alloys, AlCuMg-6, AlMgSi 1−6, and AlMg 2.5−2, as well as of a sintered aluminium powder, SAP [43] to [45].

heat-resistant material, which has an oxide content of 13 to 14 per cent, and which is used in the manufacture of semi-finished products, e.g. by extrusion or pressing [43]. The strength and deformation properties of aluminium alloys are considerably more sensitive to increase in temperature than those of steels. Even temperatures exceeding not more than 100 to 150° C give rise to a large reduction in the tensile strength, σ_B, as well as in the 0.2 per cent yield strength, $\sigma_{0.2}$, of aluminium alloys, and cause at the same time a marked increase in the ultimate elongation, δ. Some general tendencies in the effects of elevated temperatures on the strength and deformation properties of steels have been indicated in the above. The behaviour of aluminium alloys is also characterised by similar tendencies. This implies, among other things, that the tensile strength and the 0.2 per cent yield strength are affected by the temperature in a greater degree than the modulus of elasticity, and that the properties of high-strength heat-treatable aluminium alloys are influenced by temperature more than those of low-strength non-heat-treatable alloys.

At the beginning of this chapter, mention has been made of the reducing effect of heating on the strength of a composite material possessing a high

thermal inertia, such as *concrete*, on account of the internal stresses which give rise to crack formation, and which are due to differences in the linear coefficient of thermal expansion between the constituent materials, see Fig. 33 [40], [47], as well as to the fact that the temperature distribution in the test specimen is largely non-uniform because it takes a long time for the test specimen to be heated all through. This decreasing effect produced on the strength by the internal stresses, is of great importance not only during the heating of the concrete, but also during the subsequent cooling-down period. One of the consequences of this effect is the circumstance that the residual strength of the concrete is lower than its strength at elevated temperatures. Accordingly, the changes which the exposure to a fire causes in the strength and deformation properties of the concrete are dependent on the shape of the test specimen, on the size of the test specimen, on the rate of heating, and on the duration of the heating period. Other essential factors to be considered in this connection are those which have important effects on the strength of the concrete and on its resistance to deformation under ordinary climatic conditions, i.e. the curing conditions of the test specimens before the tests, the age of the specimens at testing, and the composition of the concrete, which

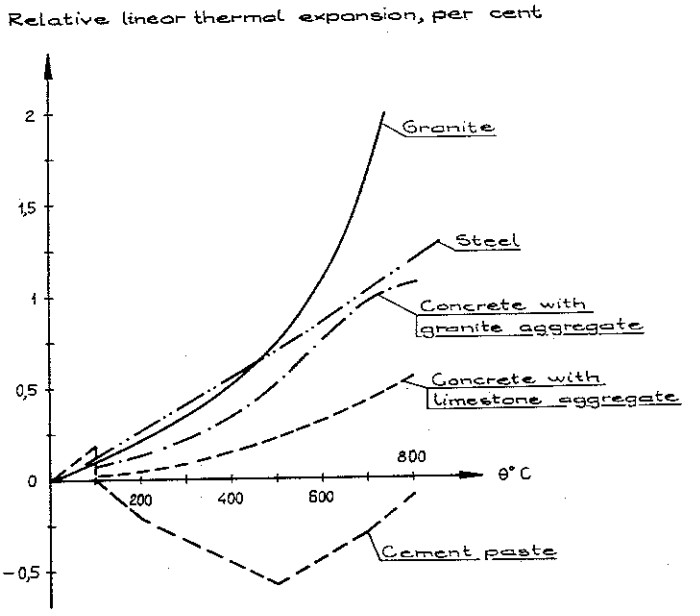

Fig. 33. Relations between the per cent linear thermal expansion and the heating temperature, θ, which are characteristic of granite, hardened cement paste, concrete made with granite aggregate, concrete made with limestone aggregate, and steel [40], [47].

involves such subfactors as the type of cement, the type of aggregate, the grading of aggregate, the water-cement ratio, and the percentage of cement paste.

Unfortunately, the present knowledge of the above-mentioned effects on the strength and deformation properties of the concrete in the temperature range associated with fires affords a highly incomplete basis for surveying the whole complex of problems under consideration, and this lays special emphasis on the need of intensified research in the field in question. The relevant results published in the literature are exemplified in Figs. 34 to 37, which represent some relations that characterise the compressive strength and the short-time modulus of elasticity of the concrete. Fig. 34 [48] relates to the concrete made with standard Portland cement, fine aggregate consisting of sand from stream deposits, and coarse aggregate consisting mainly of flint. This graph represents the effect produced by variations in the cement-to-aggregate ratio on

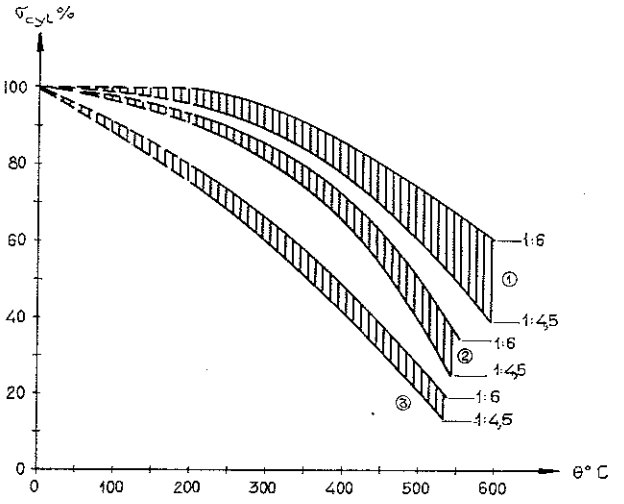

Fig. 34. Variation in the compressive strength, σ_{cyl}, with the temperature, θ, determined on concrete cylinders, 5 cm in diameter and 10 cm in length. The concrete was made with standard Portland cement, fine aggregate consisting of sand from stream deposits, and coarse aggregate consisting mainly of flint. The cement-to-aggregate ratio ranged from 1:6 to 1:4.5. The rate of heating of the concrete was 5 to 6° C per min. The curve region (1) relates to the cylinders which were subjected to a compressive load at a stress $\sigma = 73$ kp per cm² during the heating period, and were tested to failure in a heated state. The curve region (2) relates to the cylinders which were not submitted to any load during the heating period, and were tested to failure in a heated state. The curve region (3) relates to the cylinders which were not subjected to any load during the heating period, and were tested to failure after slow cooling down to 20° C [48].

the compressive strength of cylinders tested under different conditions, viz., first, cylinders subjected to a compressive stress $\sigma = 73$ kp per cm^2 and tested fo failure in a heated state (curve region 1), second, cylinders which were not loaded during the heating period, and were tested to failure in a heated state (curve region 2), and third, cylinders which were not loaded during the heating period, and were tested to failure after slow cooling down to 20° C (residual strength, curve region 3). These curves show that the per cent reduction in both the strength at high temperatures and in the residual strength increased as the cement-to-aggregate ratio became higher. Furthermore, these curves corroborate the above statement concerning a characteristic of the concrete, namely, the fact that its residual strength is lower than its strength at elevated temperatures. The effect of variations in the type of aggregate is illustrated in Fig. 35 [49] to [51], [54]. This graph represents the compressive strength determined at high temperatures on 7-cm cubes. The concrete was made with standard Portland cement and with aggregate consisting of white Jura limestone (Curve 1), basalt (Curve 2), Rhine sand (Curve 3), and crushed clinker

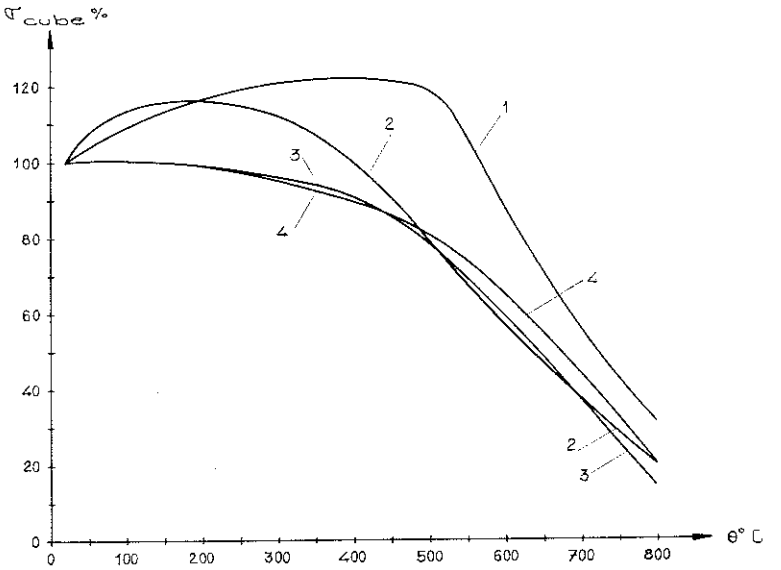

Fig. 35. Variation in the compressive strength, σ_{cube}, in a heated state and the temperature, θ, determined on concrete cubes, 7 cm in side length, which were not subjected to any load during the heating period. The concrete was made with standard Portland cement, and with aggregate consisting of white Jura limestone (Curve 1), basalt (Curve 2) Rhine sand (Curve 3), and crushed clinker (Curve 4). The test specimens were kept at the respective testing temperatures for 8 h to ensure that they had reached a steady state [49] to [51], [54].

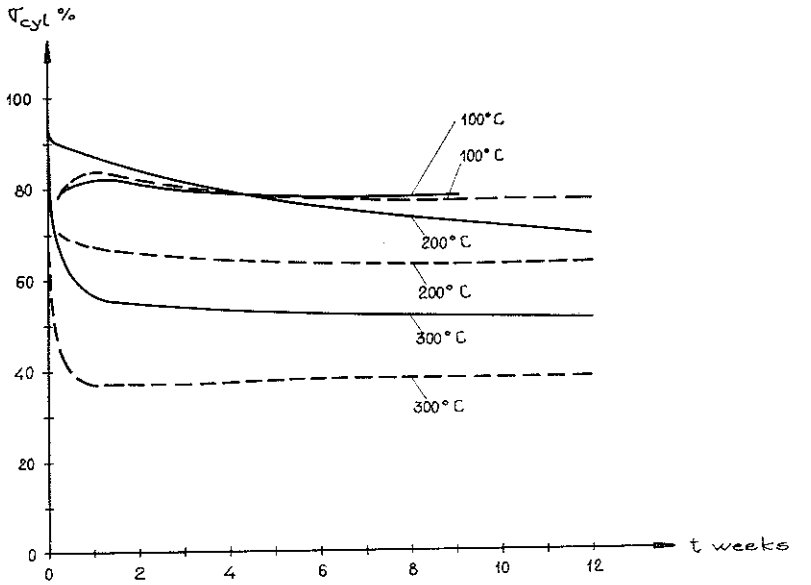

Fig. 36. Effects produced by the duration of the heating period, t, on the compressive strength in a heated state (full-line curves) and on the residual compressive strength (dash-line curves) of concrete cylinders, 5 cm in diameter and 10 cm in length, which were not submitted to any load during the heating period. The concrete was made with standard Portland cement, with fine aggregate consisting of sand from stream deposits, and with coarse aggregate consisting mainly of flint. The cement-to-aggregate ratio was 1:3 [52].

(Curve 4). As is seen from this graph, the effect of the type of aggregate is extraordinarily predominant, primarily at temperatures up to the range from 530 to 575° C, which is characterised by disintegration of $Ca(OH)_2$ and by transformation of quartz.

The duration of the heating period has a substantial influence on the strength properties of the concrete, just as on those of metallic materials. This influence is exemplified in Fig. 36 [52], which represents the effects produced by the duration of the heating period on the compressive strength at elevated temperatures (full-line curves) and on the residual strength (dash-line curves) of cylinders that were non-loaded during the heating period, and were made of concrete having a cement-to-aggregate ratio of 1:3 and consisting of the same constituent materials as those mentioned in connection with Fig. 34. It is seen from these curves that the compressive strength decreased as the duration of the heating period became greater, and that this decrease approached a limiting value. The residual strength reached this value somewhat earlier than the strength at elevated temperatures. The major part of the reduction

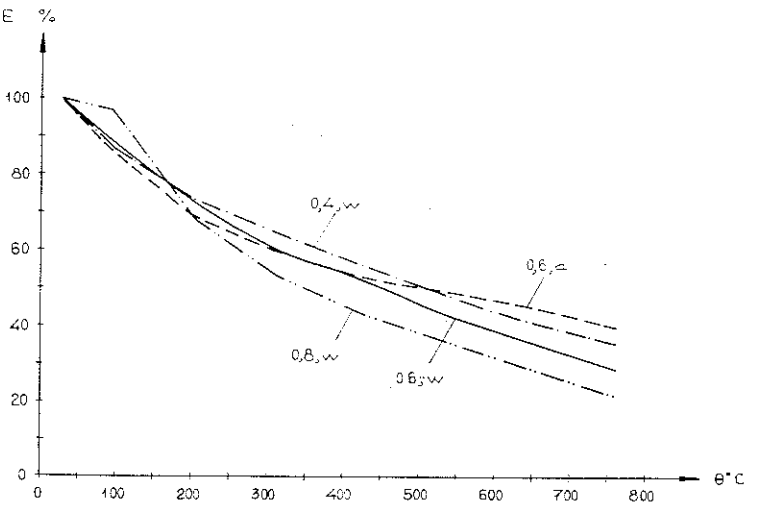

Fig. 37. Variation in the short-time dynamic modulus of elasticity in a heated state, E, with the heating temperature, θ, determined at the age of 28 days on concrete prisms, $3.8 \times 5.1 \times 15.2$ cm^3 in size, which were not subjected to any load during the heating period. The water-cement ratio was 0.4, 0.6 and 0.8. The test specimens were moist-cured for 28 days (curves marked "w"), or were moist-cured for 3 days, and then air-cured for 25 days at a relative humidity of the air of 50 per cent (curves marked "a"). The concrete was made with standard Portland cement, and with fine and coarse aggregate from Elgin, Illinois, U.S.A. [47], [53].

in strength took place during the first day of the heating period. In general, it may be considered that the reduction in strength under ordinary practical conditions comes to an end after a heating period of about 4 weeks.

A fragmentary picture of the effect of heating on the short-time modulus of elasticity, E, of the concrete is given in Fig. 37 [47], [53], which relates to tests on prisms, $3.8 \times 5.1 \times 15.2$ cm^3 in size, which were not subjected to any loads during the heating period. The concrete was made with standard Portland cement, and with fine and coarse aggregate from Elgin, Illinois, U.S.A. This graph shows how the dynamic modulus of elasticity is influenced by variations in the water-cement ratio and in the curing conditions prior to testing. As is seen from these curves, the per cent reduction in the modulus of elasticity increases at a rate that is not negligible as the water-cement ratio becomes higher. It is of interest to compare this graph with the results obtained by *Malhotra* [48], who found that the reduction in the compressive strength of the concrete caused by heating seemed to a close approximation to be independent of the water-cement ratio in the range from 0.4 to 0.65. It is furthermore seen from Fig. 37 that the modulus of elasticity of the moist-cured con-

crete test specimens was more sensitive to heating at temperatures exceeding about 400° C than that of the air-cured specimens.

As regards *lightweight concrete*, it may be noted that the knowledge of the changes caused by fires in the strength and deformation properties of this material is even more inadequate than the available information on the properties of the ordinary concrete. The scanty data on the fire resistance of lightweight concrete which are to be found in the literature are exemplified in Fig. 38 [56]. This graph relates to 9-cm Siporex cubes, which were non-loaded during the heating period, and shows the relative residual compressive strength as a function of the temperature during comparatively short heating periods. It is seen that the residual strength increased in relation to the initial strength within the temperature range extending to about 700° C. The most favourable effect on the residual strength was observed at a temperature of about 400° C. When the temperature exceeded some 700° C, the residual strength rapidly decreased. Sintering of this lightweight concrete is initiated at about 1000° C.

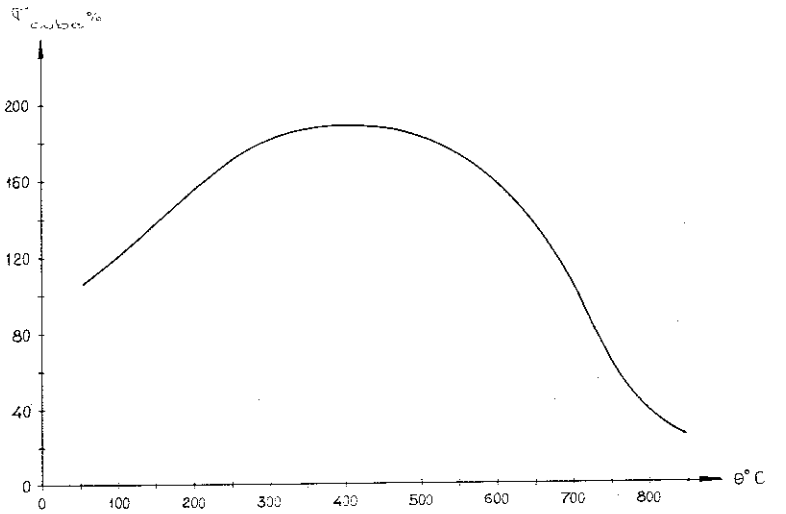

Fig. 38. Variation in the residual compressive strength, σ_{cube}, with the heating temperature, θ determined on steam-cured lightweight cement concrete cubes, 9 cm in side length, which were not submitted to any load during the heating period. Before the determination of the compressive strength, the test specimens were subjected, first, to drying out at 110° C, then to preheating for 1 to 3 h, after that to definitive heating to the respective temperatures, θ, for 4 h, and finally, to slow cooling down to ordinary room temperature [56].

6. Theoretical Calculation of Temperature Fields in, and Load-Bearing Capacity of, Load-Bearing Structures Exposed to Fires

In order to calculate the temperature fields, θ, which occur in a structure exposed to a fire, it is required to solve the equation of heat conduction (generally known as the heat equation) so as to take into account the boundary conditions which are dependent on temperature, and which are given by the coefficients of heat transfer, cf. Fig. 8, as well as by the temperatures of the air or those of the gaseous products of combustion.

In the general, three-dimensional unsteady-state case, the equation of heat conduction is, in Cartesian rectangular co-ordinates (x, y, z),

$$\frac{\partial}{\partial x}\left(\lambda_x \frac{\partial \theta}{\partial x}\right) + \frac{\partial}{\partial y}\left(\lambda_y \frac{\partial \theta}{\partial y}\right) + \frac{\partial}{\partial z}\left(\lambda_z \frac{\partial \theta}{\partial z}\right) = \gamma c_p \frac{\partial \theta}{\partial t} \tag{11}$$

and, in cylindrical co-ordinates (r, φ, z),

$$\frac{1}{r} \cdot \frac{\partial}{\partial r}\left(\lambda_r r \frac{\partial \theta}{\partial r}\right) + \frac{1}{r^2} \cdot \frac{\partial}{\partial \varphi}\left(\lambda_\varphi \frac{\partial \theta}{\partial \varphi}\right) + \frac{\partial}{\partial z}\left(\lambda_z \frac{\partial \theta}{\partial z}\right) = \gamma c_p \frac{\partial \theta}{\partial t} \tag{12}$$

where the subindices x, y, z, r, and φ affixed to the symbol of thermal conductivity, λ, indicate that these relations make it possible to take into account the varying characteristics of thermal conduction in the different co-ordinate directions.

In the case of structures exposed to fires, the solution of the heat equation is complicated by the fact that the thermal conductivity, λ, and the specific heat, c_p, vary with the temperature, θ, or with the time, t, and with the co-ordinates x, y, z or r, φ, z, respectively, in a degree that cannot be disregarded in practical calculations, cf. Figs. 20 to 24. Special complications are caused in this case by the effect of an initial moisture content on the thermal conductivity and on the specific heat, as well as by the effect produced on the specific heat by the physico-chemical changes in the material, which have been discussed at some length in the comments on Fig. 25. Figs. 39 and 40 show how important it is to take these factors into consideration in calculations of temperature fields. Fig. 39 [12] relates to a wall, one brick thick, and represents the effects which are produced by different assumptions concerning the thermal conductivity, λ, and the coefficient of heat transfer at the wall surface

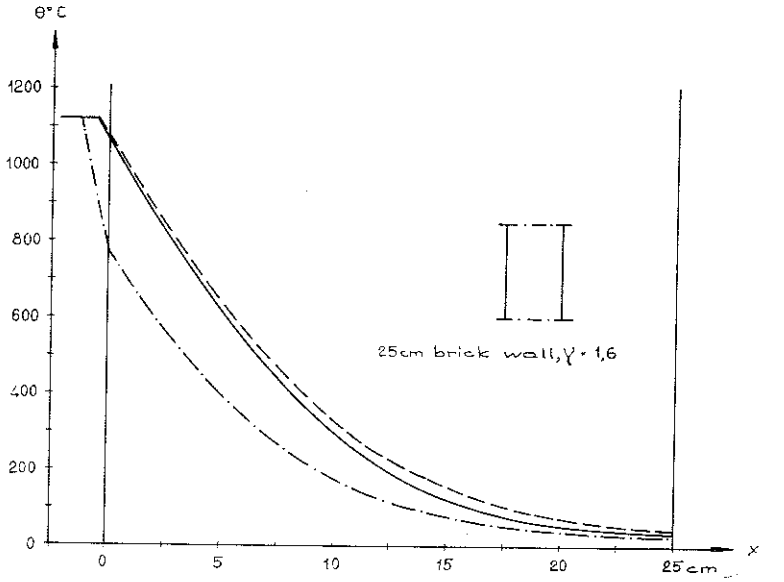

Fig. 39. Temperature fields calculated by *Ödeen* [12] for a brick wall, one brick thick (specific gravity $\gamma=1.6$), exposed on one side to a Swedish standard fire for 4 h. The full-line curve is based on the assumption that the thermal conductivity, λ, of the brick and the coefficient of heat transfer, α_e, at the wall surface exposed to the fire are dependent on the temperature. The dash-and-dot-line curve is based on the assumption that λ and α_e are independent of the temperature, and that their values are equal to those which are applicable at room temperature, viz., $\lambda=0.4$ kcal per m per h per °C and $\alpha_e=10$ kcal per m² per h per °C. The dash-line curve is based on the assumption that λ and α_e are independent of the temperature, but that their values are equal to the mean values which are representative of the temperature range under consideration, viz., $\lambda=0.5$ kcal per m per h per °C and $\alpha_e=100$ kcal per m² per h per °C. The specific heat is assumed in all cases to be independent of the temperature, and to be equal to 0.22 kcal per kg per °C.

exposed to the fire, α_e, on the temperature distribution corresponding to the exposure to a fire for 4 h under the conditions specified in the relevant Swedish standards. Fig. 40 [31] represents the effect of variations in the initial moisture content on the fire endurance, i.e. the fire resistance period, of brick walls differing in thickness.

For the case where the thermal conductivity and the specific heat do not vary with the temperature, many publications, e.g. [57] to [63], give analytic solutions of the equation of heat conduction applied under unsteady-state conditions to homogeneous structures which are simple in design, and which involve simple boundary conditions. On the other hand, the problem of heat conduction under unsteady-state conditions in the case where the thermal conductivity and the specific heat vary with the temperature is mathematically

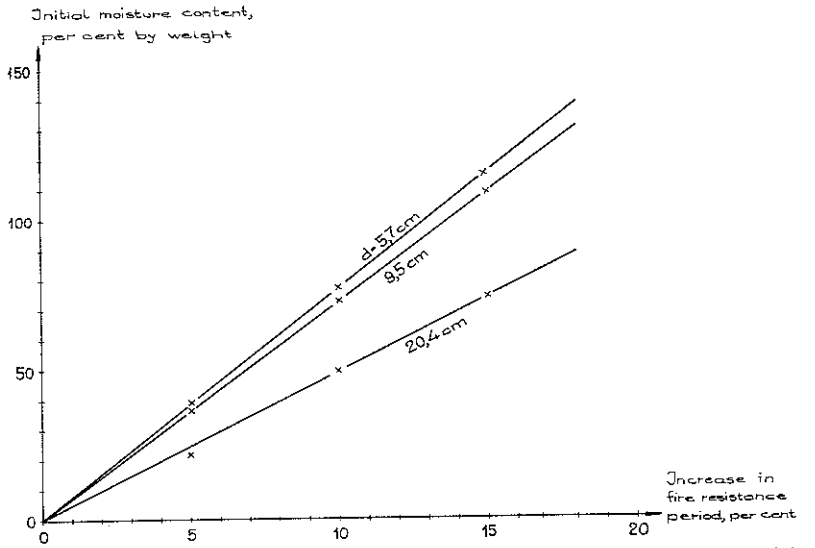

Fig. 40. Relation between the per cent increase in the fire resistance period of a brick wall of varying thickness, d, exposed to the fire on one side and the initial moisture content. These curves were calculated by *Harmathy* [31]. The results represented in this graph take into account the variation in the thermal conductivity and in the specific heat of brick with the temperature. The fire resistance period, as defined in this connection, is the interval from the beginning of a standard fire to the instant at which the temperature on the unexposed face of the wall reaches 250° F (121° C).

more complicated, and analytic solutions of this problem have been dealt with in the literature only to a small extent. At the same time, these solutions have been limited to cases based on highly idealised and simplified assumptions [64]. The solutions in question are very intricate, and are extremely laborious when they are used as a basis for practical calculations applied to fire engineering problems.

At the present time, numerical data processing by means of electronic computers offers a practicable procedure which enables the temperature fields due to the effects of fires on structures to be calculated so as to take account of the variations in the thermal characteristics of materials with the temperature, and which requires a reasonable amount of work. It is natural that such numerical data processing is based on linear difference equations which are deduced for a structure divided into elements. In the case of one-dimensional heat conduction under unsteady-state conditions, these equations have the form [2], [12], [24], cf. Fig. 41,

$$\varphi_1 \frac{\Delta\theta_1}{\Delta t} = \psi_1(\theta_e - \theta_1) - \psi_2(\theta_1 - \theta_2)$$

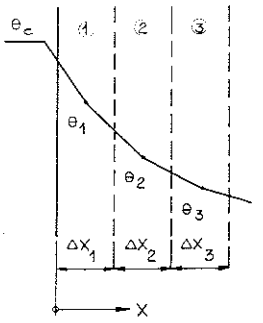

Fig. 41. Division of a structure into elements for use in the difference equations dealing with one-dimensional heat conduction under unsteady-state conditions [2], [12], [24].

$$\varphi_2 \frac{\Delta\theta_2}{\Delta t} = \psi_2(\theta_1 - \theta_2) - \psi_3(\theta_2 - \theta_3) \tag{13}$$

etc.,

where

$$\varphi_1 = c_{p1}(x, \theta) \cdot \gamma_1(x, \theta) \cdot \Delta x_1$$

$$\varphi_2 = c_{p2}(x, \theta) \cdot \gamma_2(x, \theta) \cdot \Delta x_2 \tag{14}$$

and

$$\psi_1 = \frac{1}{\frac{1}{\alpha_e(\theta)} + \frac{\Delta x_1}{2\lambda_1(x, \theta)}}$$

$$\psi_2 = \frac{1}{\frac{\Delta x_1}{2\lambda_1(x, \theta)} + \frac{\Delta x_2}{2\lambda_2(x, \theta)}}$$

$$\psi_3 = \frac{1}{\frac{\Delta x_2}{2\lambda_2(x, \theta)} + \frac{\Delta x_3}{2\lambda_3(x, \theta)}} \tag{15}$$

Figs. 42 and 43 exemplify the temperature fields calculated with the help of electronic data processing by the aid of the method outlined in the above. Fig. 42 illustrates the temperature conditions characterising a concrete wall, 15 cm in thickness, which is either non-insulated or insulated with lightweight concrete on the side that is not exposed to the fire, when its opposite face is

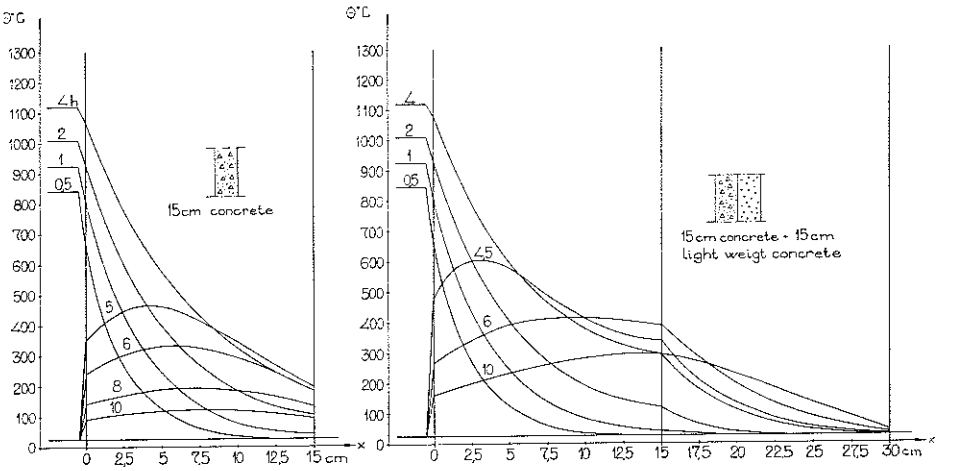

Fig. 42. Calculated temperature fields in a concrete wall exposed on one side to a Swedish standard fire for 4 h. Each curve is marked with a number expressing the length of exposure to the fire (0.5 to 10 h).

(a) Non-insulated concrete wall, 15 cm in thickness.

(b) Concrete wall, 15 cm in thickness, insulated with lightweight concrete (specific gravity $\gamma=0.5$), 15 cm in thickness, on the unexposed face. These temperature fields were computed on the assumption that the temperature in the enclosed room varies in accordance with the Swedish standard temperature-time curve during 4 h, and then falls instantaneously to +20°. *Ödeen* [12].

exposed to a Swedish standard fire for 4 h. This graph shows, among other things, the marked effect of the lightweight concrete insulation in preventing heat transfer, with the result that the insulated concrete wall has to withstand higher temperatures than the non-insulated wall. Fig. 43 illustrates an application of the method in question to a problem of heat conduction in a cylindrical, axially symmetrical body. This graph represents the calculated temperature-time curves which characterise a steel suspender provided with mineral wool insulation varying in thickness, d, and subjected to a Swedish standard fire for 1/2 h and for 3/4 h.

At present, calculated temperature fields and the available information on the variations in the properties of materials with the temperature can serve as a basis for an approximate determination of the load-bearing capacity of a structure at different instants throughout the duration of a fire in special cases, such as statically determinate steel structures and those statically determinate reinforced concrete structures in which failure is initiated by yielding of the reinforcement. On the other hand, it is not possible for the time being to calculate by means of the corresponding theoretical methods the ultimate

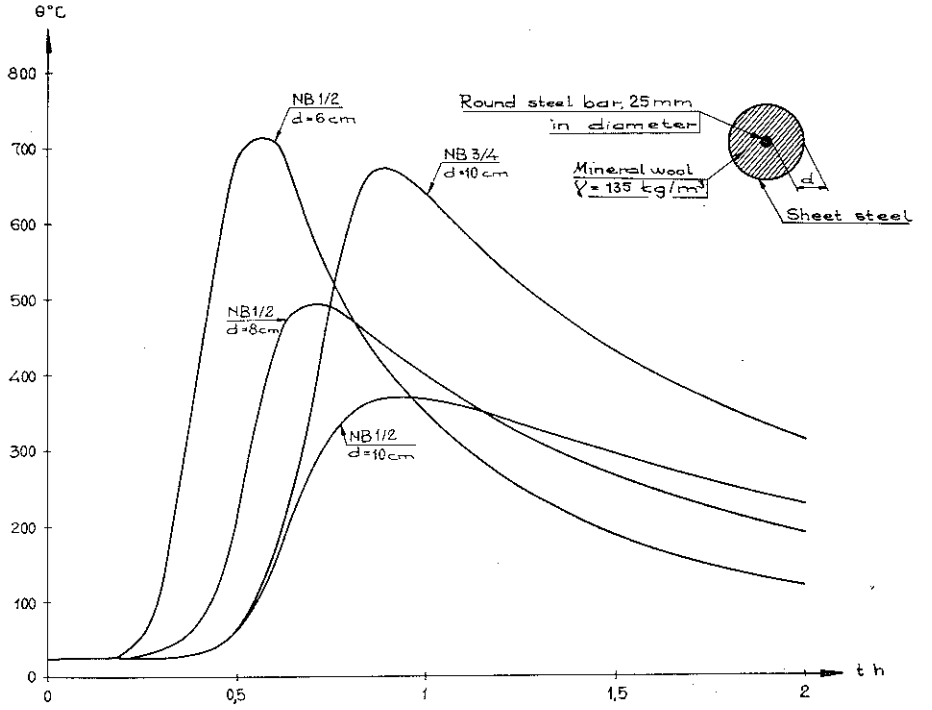

Fig. 43. Calculated temperature-time curves corresponding to exposures of $\frac{1}{2}$ and $\frac{3}{4}$ h (marked NB ½ and NB¾, respectively) to a Swedish standard fire and relating to a steel suspender, 25 mm in diameter, insulated with a layer of mineral wool (weight per unit volume, γ=135 kg per m³) of thickness d cm which was enclosed in sheet steel in order to reduce the effect of convection. These curves were computed on the assumption that the temperature in the enclosed room varies in conformity with the Swedish standard temperature-time curve during $\frac{1}{2}$ and $\frac{3}{4}$ h, respectively, and then falls instantaneously to +20° C.

loads of statically indeterminate structures. Their behaviour under the action of fires is to be described as unexplored, and hence to be regarded as one of the most urgent subjects which should be taken up without delay in structural fire engineering research.

The fire resistance of load-bearing steel, concrete, and timber structures is briefly discussed under some aspects in what follows.

6.1. Fire Resistance of Load-Bearing Steel Structures

From the above considerations on the process of fire development as well as on the thermal properties and strength and deformation characteristics of structural materials, it may be inferred that in order to prevent a load-bearing

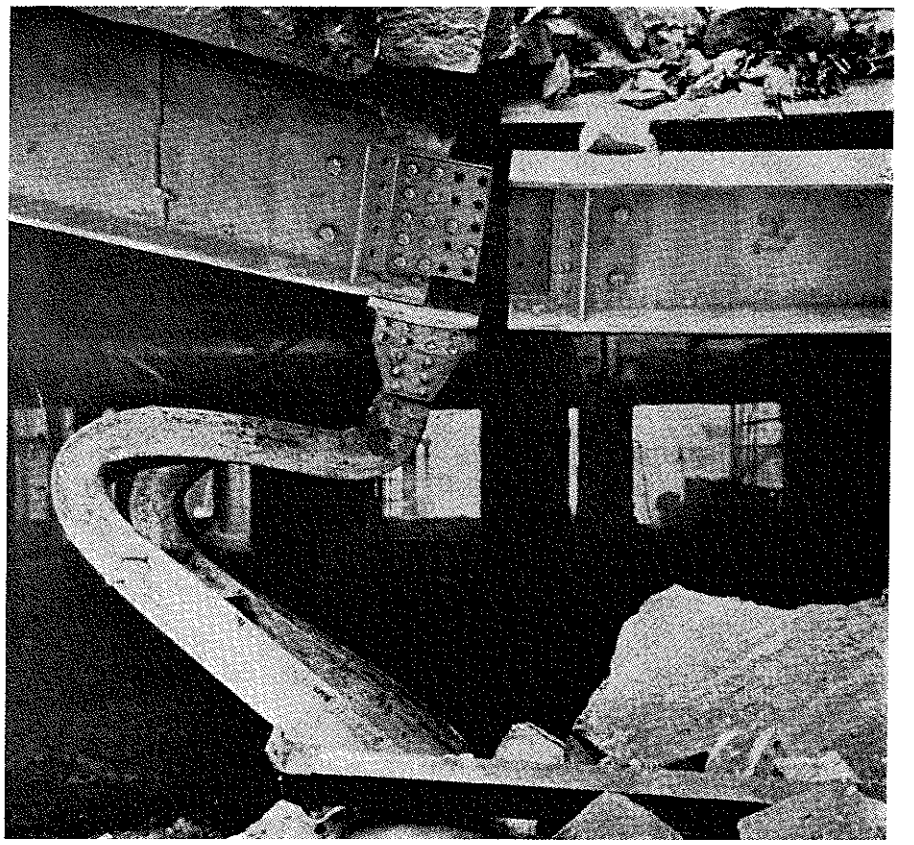

Fig. 44. Non-insulated load-bearing steel column which has collapsed after a short-time exposure to a fire [65].

steel structure from collapsing in case of fire – if we abstract from fires of very short duration – such a structure must be provided with insulation in some form or other, which retards the temperature rise in the steel. For determining the insulation required in such cases, the designer of today has at his disposal special lists which have been drawn up on the basis of fire tests, and which show the thicknesses of insulation corresponding to various materials and to different fire grading classes. All these thicknesses have been determined from a condition which states that a steel structure protected by the insulation shall be assumed to collapse when the temperature in this structure reaches a certain definite value – cf. in this respect Fig. 45. This graph, which has been published by *Boué* [7], is based on a critical steel temperature of 400° C. The critical temperature of steel varies not inconsiderably from one country

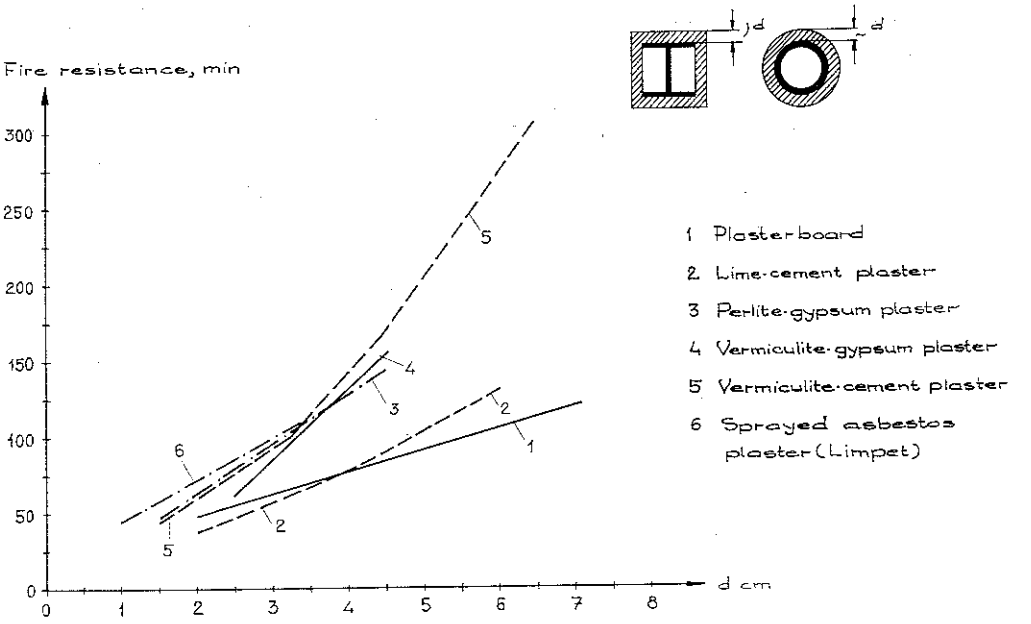

Fig. 45. Fire resistance of steel columns provided with fire-resistive insulation of thickness d cm consisting of plasterboard (Curve 1), lime-cement plaster (Curve 2), perlite-gypsum plaster (Curve 3), vermiculite-gypsum plaster (Curve 4), vermiculite-cement plaster (Curve 5), and sprayed asbestos plaster (Curve 6). This graph is based on the temperatures of the steel observed in fire tests, and was plotted on the assumption that the critical temperature of the steel is 400° C. *Boué* [7].

to another, but is taken in each individual country to be a constant quantity, which is independent of the type of failure and of the magnitude of the working stress.

Fire engineering design of load-bearing steel structures based on these general principles, which are conventionally applied at the present time, involves an excessive simplification of the problem under consideration. It is seen from Fig. 27 that the critical steel temperature of a load-bearing steel structure varies to a non-negligible extent with the magnitude of the working stress which acts on the structure during the fire, and which can be subject to substantial changes in the course of the process of fire development. These changes can be due to a reduction in the load or, on the contrary, to the occurrence of temperature stresses, which are set up when the thermal expansion is partially or completely prevented. As is furthermore seen from Fig. 27, the decrease in the yield point stress, σ_s, with increase in the temperature takes place at a considerably higher rate than the reduction in the modulus of elas-

ticity, E, with the result that the critical temperature of steel is also dependent on the type of failure.

A natural development of the present, largely schematised method of fire engineering design of steel structures consists in replacing it by a more refined procedure, which is based in each individual case on the working stress met with in this case, on the available curves representing the variations in the strength and deformation properties of the material in question with the temperature, as well as on the temperature-time curves of the load-bearing steel structure calculated with reference to the characteristics of combustion in the case under consideration. Such temperature-time curves can be calculated to a satisfactory degree of accuracy by means of electronic data processing if use is made of the procedure outlined in the above, cf. Fig. 43. Moreover, it is found from the literature that approximate methods, which are satisfactory under ordinary practical conditions, have been devised for determining the temperature, θ_s, which is reached in a fire-protected steel structure exposed to a fire [8], [66], [67]. These methods take account of the effects due to the thermal inertia characteristics of the protective insulation and the steel structure. The methods in question can be exemplified by the following approximate relation, which has been deduced in [67]:

$$\theta_s = 1325\left[1-e^{-\frac{t-t_1}{RQ}}\right]+\frac{430e^{-0.2t_1}}{1-0.2RQ}\left[e^{-\frac{t-t_1}{RQ}}-e^{-0.2(t-t_1)}\right]+$$

$$+\frac{270e^{-1.7t_1}}{1-1.7RQ}\left[e^{-\frac{t-t_1}{RQ}}-e^{-1.7(t-t_1)}\right]+\frac{625e^{-19t_1}}{1-19RQ}\left[e^{-\frac{t-t_1}{RQ}}-e^{-19(t-t_1)}\right] \quad (16)$$

This relation is based on the assumption that the temperature in the enclosed room exposed to the fire, θ_b, varies in accordance with the equation

$$\theta_b-\theta_0=\bar{F}(t)=1325-430e^{-0.2t}-270e^{-1.7t}-625e^{-19t} \quad (17)$$

which describes to a fairly high degree of accuracy the temperature-time curve that has been proposed as an international standard, cf. Fig. 46. The notations used in Eq. (16) are

$$Q=Q_s+Q_i+Q_l \quad (18)$$

$$Q_s=\gamma_s A_s c_{ps} \quad (19)$$

$$Q_i=\tfrac{1}{3}\gamma_i d_i o_i c_{pi} \quad (20)$$

$$Q_l=V_l\bar{c}_{pl} \quad (21)$$

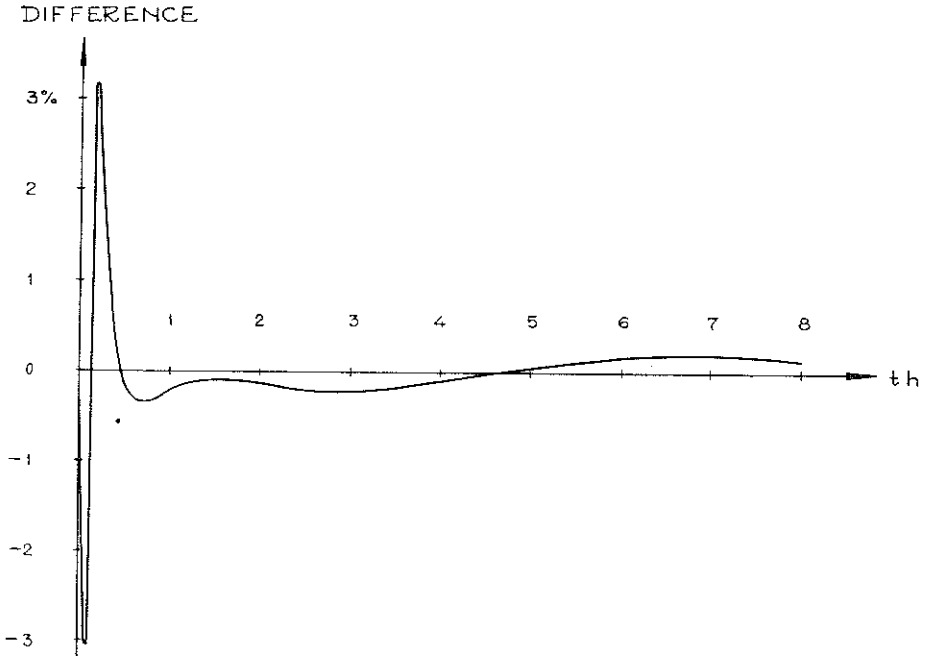

Fig. 46. Difference between fire temperature of an enclosed space, $\bar{F}(t)$, calculated according to Eq. (17), and corresponding temperature according to ISO/TC 92, INSTA 28/2, or DIN 4102—62 standard curve [67].

$$R=\frac{d_i}{\lambda_i o_i} \tag{22}$$

$$t_1=\tfrac{1}{2}RQ_i \tag{23}$$

where

γ_s = the weight per unit volume of the steel,
A_s = the cross-sectional area of the steel structure,
c_{ps} = the specific heat of the steel,
γ_i = the weight per unit volume of the insulating material,
d_i = the thickness of the insulation,
o_i = the perimeter of the insulation,
c_{pi} = the specific heat of the insulating material,
λ_i = the thermal conductivity of the insulating material,
V_l = the volume of the air entrapped per unit length in the interspace between the insulation and the steel structure,
$\bar{c}_{pl}$ = the specific heat per unit volume of the air.

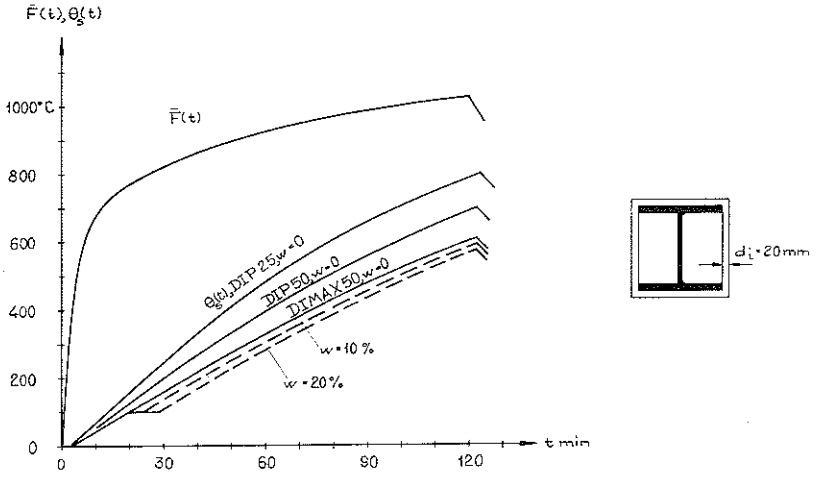

Fig. 47. Curve determined from Eq. (17) and representing the variation in the temperature in an enclosed room, $\bar{F}(t)$, with the time under exposure to a fire for 2 h, and the corresponding curves calculated from Eq. (16) and representing the variation in the temperature of the steel, θ_s, with the time in a steel column made of a DIN standard structural shape Dip 25, Dip 50, or Dimax 50, and insulated with a layer of vermiculite-cement plaster, 20 mm in thickness. W is the initial moisture content of thet proective insulation, in per cent by weight.

A concrete application of the approximate relation given by Eq. (16) is shown in Fig. 47 [67], which represents the variations in the steel temperature, θ_s, in the case of a steel column made of a DIN standard structural shape Dip 25, Dip 50, or Dimax 50, and insulated with a layer of vermiculite-cement plaster, 20 mm in thickness, which was exposed to a Swedish standard fire for 2 h. These curves demonstrate, among other things, that the temperature rise was manifestly dependent on the thermal inertia of the steel column, whereas this factor is disregarded in the conventional methods of fire engineering design which are in use at the present time.

6.2. Fire Resistance of Load-Bearing Reinforced Concrete Structures

As has been pointed out in the above, the available knowledge of the variations in the strength properties of reinforcing steels with the temperature makes it possible today to use a calculated temperature field associated with the exposure to a fire as a basis for computing the load-bearing capacity of those statically determinate reinforced concrete structures whose failure is initiated by yielding of the reinforcement. These assumptions are complied with in statically determinate reinforced concrete beams which are liable to

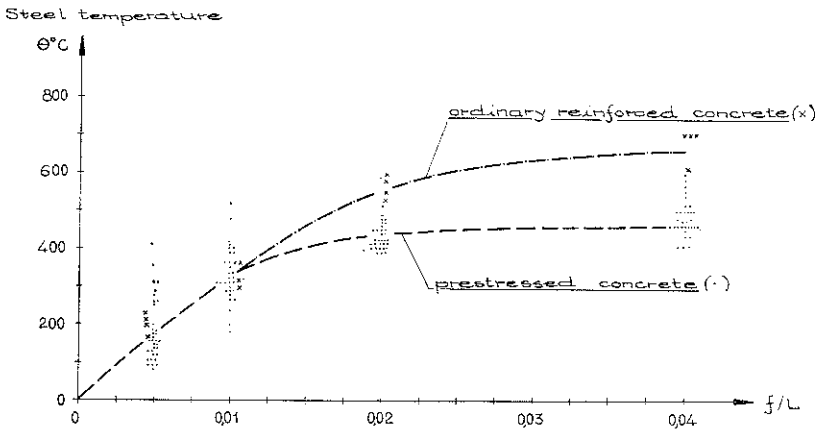

Fig. 48. Average curves representing the relation between the temperature of the reinforcement, θ, and the ratio of the deflection at the centre of the beam, f, to its span length, L. These curves were determined from extensive test series on reinforced concrete beams and prestressed concrete beams, which were simply supported at both ends, and were subjected to the maximum permissible uniformly distributed loads [41].

failure in flexure. In this respect, it is useful to examine Fig. 48, which relates to reinforced concrete beams and to prestressed concrete beams. This graph reproduces average curves representing the relation between the temperature of the reinforcement and the deflection at the centre of the beam. The curves were determined from extensive test series on concrete beams which were simply supported at both ends, and were submitted to the maximum permissible uniformly distributed loads [41].

In spite of the fact that there is an obvious need for a systematic survey which would show how the fire resistance of reinforced concrete beams of various types subjected to flexural loads is influenced by variations in the cross-sectional area, in the cross-sectional shape, in the concrete cover of the reinforcement, in the distribution of the reinforcement over the cross section, and in the number of surfaces exposed to the fire, and notwithstanding the available possibilities of a theoretical numerical treatment of this problem under statically determinate conditions, no theoretical study of this kind has to the Author's knowledge – been published in the literature up to now. It is probable that this deficiency is primarily due to difficulties involved in a theoretical numerical treatment of two-dimensional or three-dimensional heat conduction under unsteady-state conditions. In connections with fires, these difficulties are accentuated by the fact that it is necessary to take into account the variations in the thermal conductivity and in the specific heat, and also,

when required, to take into consideration the initial moisture content and the changes caused by heating in the physico-chemical properties of materials. This state of affairs emphasises the urgent need of extensive research in the field under review. It appears advisable to concentrate this research work on two main objectives. In the first place, it is necessary to investigate as many-sidedly as possible the factors which produce substantial effects on the fire resistance of reinforced concrete beams subjected to bending. Nowadays, such investigations can be carried out by treating the difference equations of heat conduction with the help of electronic computers. In the second place, it is required to evolve approximate methods which are suited for practical estimates of the load-bearing capacity corresponding to a given process of fire development.

For those statically determinate reinforced concrete structures whose failure in case of exposure to a fire is primarily determined by the strength and deformation properties of the concrete, no methods are available at the present time for computing their load-bearing capacity on the basis of calculated temperature fields. Similarly, no corresponding methods have been devised for dealing with statically indeterminate reinforced concrete structures – neither when their failure is primarily governed by the properties of the concrete, nor when the properties of the reinforcement are the foremost decisive factors in determining failure. These problems are considerably complicated by the internal stresses which are set up because the temperature distribution in the structure is markedly non-uniform since the concrete is heated through at a slow rate, and which are difficult to determine by calculation. The problems relating to statically indeterminate structures are moreover substantially complicated by the temperature moments which are produced by heating when the deformations are partly or wholly prevented, and which change in the course of fire development owing to cracking, plastification, structural transformations of the concrete, and to other causes. Up to now, these temperature moments have been studied in a very limited extent. As has already been pointed out in the above, the need of research work required for elucidating these phenomena is to be regarded as extremely urgent.

The information available today on the fire resistance and on the static behaviour or reinforced concrete structures of various types exposed to fires is based on results of standard fire tests. Normally, a few isolated fire tests are made on a structure or a structural part representing a special individual design, whereas the literature contains but a small number of reports on relatively extensive systematic fire test series carried out with a view to studying more thoroughly the behaviour of a structural system or a structural type under exposure to fire. The results obtained from such comparatively extensive

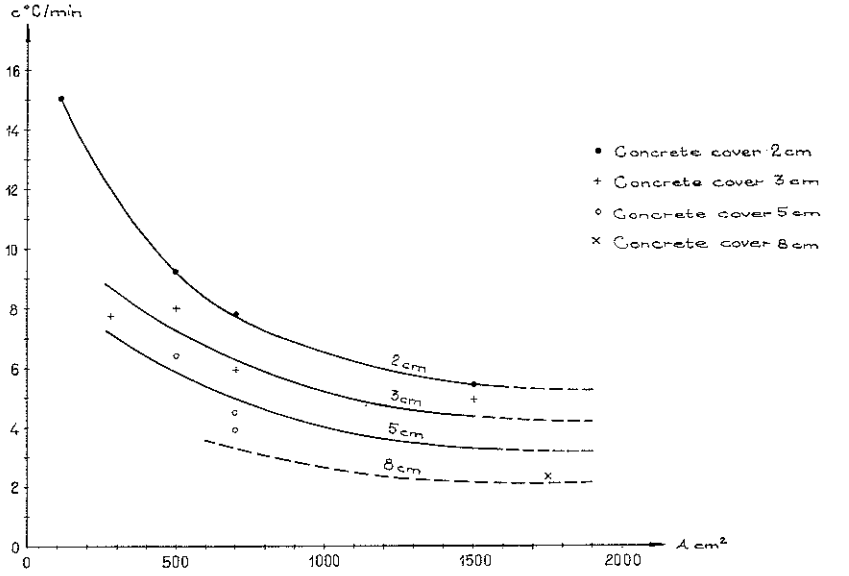

Fig. 49. Variation in the rate of heating, c, of the reinforcement in prestressed concrete beams of rectangular and I cross section with the cross-sectional area of the beam, A, and with the concrete cover of the reinforcement. This graph is based on results of British and Dutch fire tests [41].

test series on reinforced concrete structures are exemplified in Figs. 49 to 51. Fig. 49 [41] is based on British and Dutch fire tests, and shows how the rate of heating, c, of the reinforcement in prestressed concrete beams of rectangular and I cross section varies with the cross-sectional area of the beam, A, and with the concrete cover of the reinforcement. These results relate to beams whose undersurface and lateral surfaces were exposed to the fire, and whose tendons were placed in such a way that the distances from all tendons to the exterior faces of the beam were approximately equal. The test results reproduced in this graph are very valuable in themselves, but it should be observed that one of the essential parameters entering into the problem under study has been disregarded. This parameter is the shape of the cross section, which may be represented, for instance, by the ratio of the cross-sectional area to that portion of the perimeter which is exposed to the fire. Fig. 50 [68] reproduces the design charts based on the results of British fire tests dealing with square reinforced concrete columns, which were subjected to axial compressive loads under such conditions that the risk of buckling was negligible, and were exposed to the fire on all lateral surfaces. These design charts can be used to determine the load-bearing capacity, P_u, by means of the approximate relation

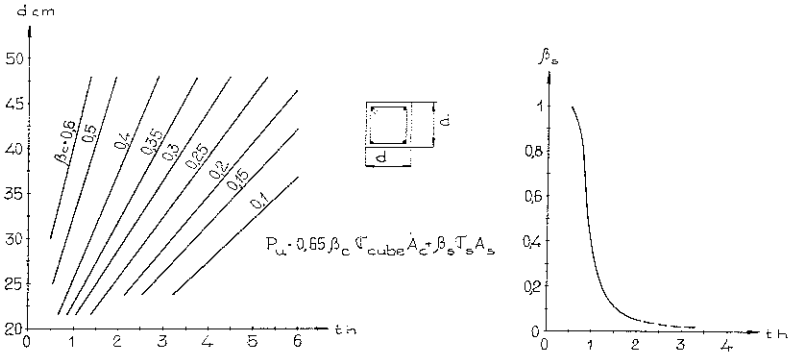

Fig. 50. Coefficients β_c and β_s entering into Eq. (24), which expresses the load-bearing capacity, P_u, of square reinforced concrete columns subjected to axial compressive loads and exposed to the fire on all lateral surfaces. These design charts are based on results of British fire tests, in which the concrete was made with standard Portland cement and with coarse aggregate consisting of gravel. These charts are applicable on condition that the vertical reinforcing bars are placed in the corners of the cross section, and that the thickness of the non-reinforced concrete cover is comprised within the approximate range from 20 to 40 mm [68].

$$P_u = 0.65\beta_c\sigma_{cube}A_c + \beta_s\sigma_s A_s \tag{24}$$

where

A_c = the cross-sectional area of the concrete,

A_s = the total cross-sectional area of the vertical reinforcing bars,

σ_{cube} = the compressive strength of the non-heated concrete, determined on 20-cm cubes, which are cured under standard conditions,

σ_s = the yield point stress of the vertical reinforcing bars, determined on non-heated test specimens,

β_c, β_s = the dimensionless coefficients represented in Figs. 50 a and 50 b, respectively; these coefficients express the reduction in the load-bearing capacity of the concrete cross section and in that of the vertical reinforcing bars, respectively, under the action of a standard fire of varying duration, t.

The relation given in Eq. (24), together with the requisite charts representing the coefficients β_c and β_s, has been verified by tests where the lateral dimension, d, varied from 20 to 48 cm, and where the concrete cover of the vertical reinforcing bars placed in the corners of the cross section varied in thickness from 22 to 38 mm. This relation can be used to calculate either the load-bearing capacity, P_u, corresponding to a given column design and to a given duration of the fire, or the duration of the fire at which a column of a given

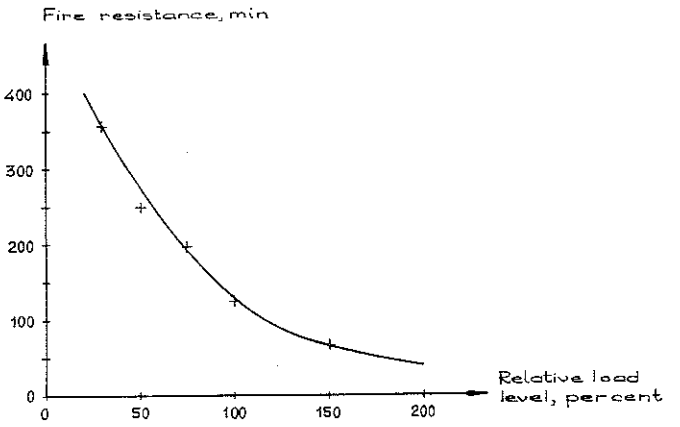

Fig. 51. Relation between the fire resistance and the relative load level. This curve, which was calculated from Eq. (24), refers to a square reinforced concrete column which is subjected to an axial compressive load, and is exposed to the fire on all lateral surfaces. Design data: $d=38.1$ cm, $A_s=25.7$ cm² (4 reinforcing bars, 28.6 mm in diameter), $A_c=1426$ cm², $\sigma_s=2200$ kp per cm², and $\sigma_{cube}=265$ kp per cm². The 100-per-cent relative load level chosen in this case is $P_u=100$ Mp, and corresponds to one-third of the load-bearing capacity of the column before the fire. The points marked with + represent the results obtained from British fire tests [53], [68] on columns which were closely similar in design to that assumed in these calculations.

design will collapse under a given load. This method enables several factors to be taken into account in a differentiated manner, viz., the quality of concrete, the quality of reinforcement, the lateral dimension of the cross section, the percentage of reinforcement, the load level, and the duration of the fire. The application of this method in an individual case is illustrated in Fig. 51, which represents the relation between the load level and the fire resistance calculated from Eq. (24) for a given column design. For comparison, this graph also shows the results obtained from fire tests [53], [68] on a column which was closely similar in design to that assumed in the calculations.

6.3. Fire Resistance of Load-Bearing Timber Structures

Timber structures, as distinguished from steel and reinforced concrete structures, are in a class by themselves, e.g. in that they are combustible. Consequently, the fire endurance of small-sized load-bearing timber structures is low. For instance, after the exposure to a fire for 10 min, the load-bearing capacity of a timber board, 1 in. by 4 in. in size, subjected to bending in the direction of maximum rigidity equals only about 5 per cent of its initial value [71]. On the other hand, since the time taken for the fire to burn through a

structure increases as the dimensions of the structure become larger, and since the non-charred portion of the cross section of the structure has a good ability to withstand stresses, the fire resistance of load-bearing timber structures of large dimensions is considerable.

The studies of the fire resistance of load-bearing timber structures which have been published in the literature deal in the main with solid and glued laminated beams and columns. Extensive American, British, Danish, Finnish, German, Japanese, and Swedish investigations of structural members of these types have shown that the rate of increase in the depth of the charred layer

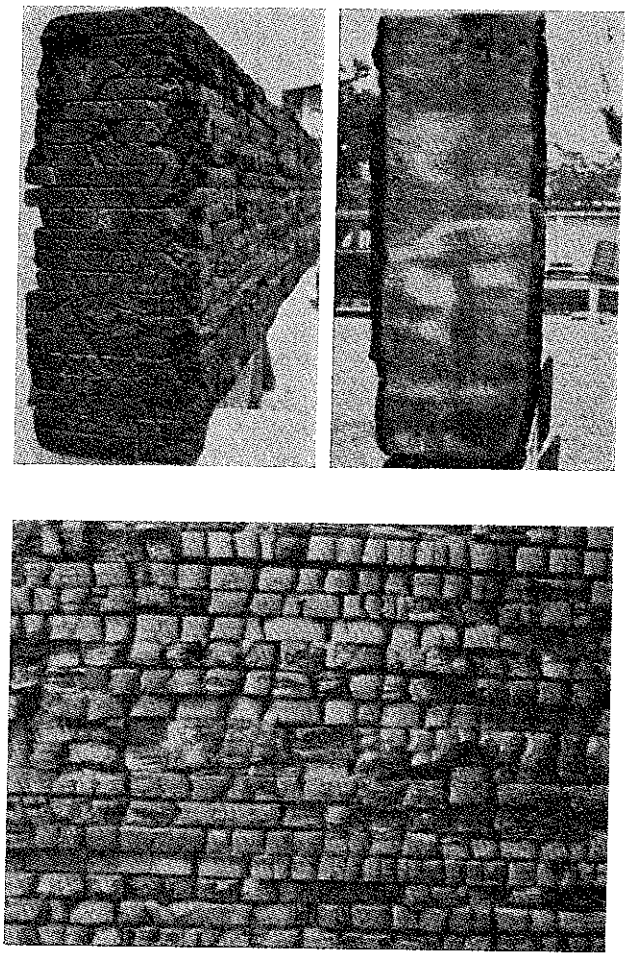

Fig. 52. Effect of a 30-min fire on a glued laminated spruce beam of rectangular cross section having the dimensions 18 by 45 cm² before the fire [70].

formed in the course of a fire is to a close approximation constant when the duration of the fire does not exceed about 2 h [69] to [71]. The rate of increase in the depth of the charred layer ranges from 0.5 to 0.7 mm per min for fir beams and columns, and amounts to about 0.4 mm per min when these structural members are made of oak or teak. This rate is approximately the same for solid and glued laminated timber structures, and is practically independent of the thickness of the laminations within the range of variation covered in the above-mentioned investigations, which extended from 18 to 34 mm.

In fir and oak structures, the charred layer formed by combustion is characterised by adequate adhesion and by satisfactory resistance to mechanical action, e.g. due to sprinkling with water, whereas the charred layer on teak is brittle, and separates easily from the uncharred wood. Owing to its relatively high heat-insulating power (thermal conductivity $\lambda = 0.05$ to 0.07 kcal per m per h per °C), a charred layer that remains on the uncharred wood considerably retards the temperature rise in the sound portion of the structure, and substantially reduces the supply of oxygen which is required for sustained combustion. The temperature rise in the uncharred portion of the structure is furthermore materially retarded owing to the fact that the water which is initially contained in the timber, as well as the additional water which is formed by pyrolysis, moves during the development of fire towards the interior portions of the cross section, and causes in these portions an increase in the moisture content, which has been demonstrated experimentally. A combined effect of all these factors is a very slow temperature rise in the uncharred parts of a timber structure exposed to a fire. This can be illustrated by the results of the investigations published by *Holm* [71], which dealt with timber beams exposed to the fire on all their lateral surfaces. The temperatures observed at the centres of the cross sections in the measurements made on laminated fir beams, 14 by 24 cm² and 16 by 36 cm² in cross section, as well as on solid fir beams, 16 by 34 cm² and 16 by 36 cm² in cross section, amounted to about +25° C after a 30-min fire test, and ranged from +65 to +75° C after a 60-min fire test.

If it is assumed that the increase in the depth of the charred layer per unit time is constant, and that the strength properties of the uncharred portion of the cross section are the same as those of the timber before the exposure to the fire, then it is not difficult to deduce relations for calculating the load-bearing capacity of statically simple load-bearing timber structures at any given instant of a process of fire development. In the case of glued laminated rectangular timber beams of width B and depth D subjected to bending, this problem has been dealt with by *Imaizumi* [70], [71]. He assumed that the rate of increase in the depth of the charred layer which is representative of spruce

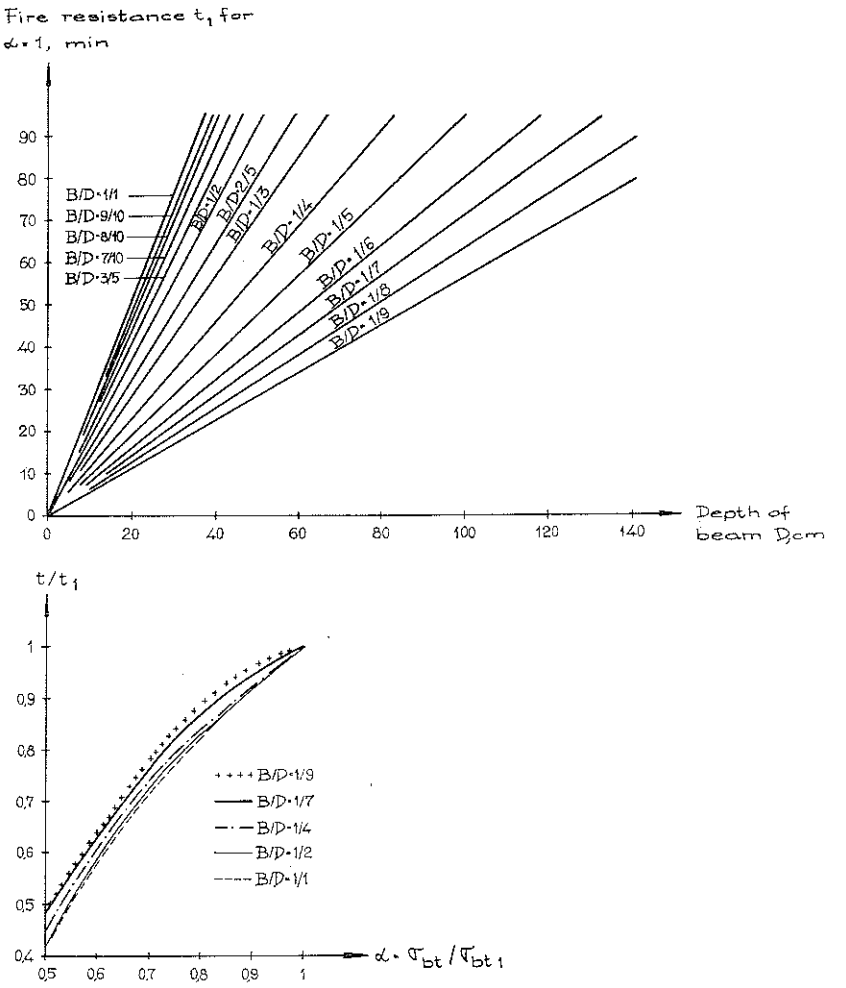

Fig. 53. Graphs calculated by *Imaizumi* [70], [71] for determining the fire resistance, t, of glued laminated spruce beams of rectangular cross section subjected to flexural loads and exposed to the fire on all lateral surfaces. The width and the depth of the beam before the fire are denoted by B and D, respectively. These graphs are based on the assumption that the rate of increase in the depth of the charred layer is 0.6 mm per min, and that the bending moment acts on the beam in the direction of its maximum rigidity, and amounts to one-third of the corresponding ultimate moment of the cross section of the beam before the fire. The ratio of the flexural compressive strength of the uncharred portion of the beam at a given instant of the process of fire development, σ_{bt}, to the initial flexural compressive strength of the beam before the fire, σ_{bt1}, is denoted by α. The fire resistance corresponding to $\alpha=1$ is designated by t_1 in Fig. 53 a.

is 0.6 mm per min. His results are exemplified in Fig. 53 a, which represents the calculated relation between the beam dimensions, B and D, before the fire and the fire resistance, t_1, defined as the time after which the bending moment of the uncharred portion of the beam is equal to one-third of the initial ultimate bending moment of the beam. This fire resistance can be corrected so as to take into account that reduction in the flexural compressive strength of the uncharred portion of the cross section which is caused by heating and by increased moisture content. For this purpose, *Imaizumi* has given the curves, reproduced in Fig. 53 b and based on the ratio, α, of the flexural compressive strength, σ_{bt}, of the uncharred portion of the cross section at a given instant of the process of fire development to the flexural compressive strength, σ_{btl}, of the beam under the initial conditions before the fire. In dealing with beams which are slender in a lateral direction, a calculation of the fire resistance corresponding to failure in pure flexure based on the curves shown in Figs. 53 a och 53 b must ordinarily be supplemented with an analogous calculation in order to check the design with respect to the risk of failure in lateral buckling. However, no method which would be suited for practical calculations with a view to checking beam designs for lateral buckling under such conditions has so far been published in the literature.

At the present time, the greatest difficulty encountered in calculations of the fire resistance by means of the procedure described in connection with Fig. 53 is the correct choice of the value of the parameter α [69], [71] in each individual case. This choice necessitates detailed information on the temperature and moisture distributions which occur in uncharred portions of structures exposed to fires, as well as on the effects produced by variations in the moisture content and in the temperature on the strength properties of timber. Some isolated investigations have shown that a temperature rise from 20 to 100° C causes a reduction of up to about 50 per cent in the flexural compressive strength of firewood. It is to be noted, however, that this question has been explored extremely little up to now, and is therefore entitled to a high priority among urgent problems in structural fire engineering research. Other studies which also deserve a high priority in the field of load-bearing timber structures are those which deal with the effects of fires on the behaviour of such structures as load-bearing timber trusses and nailed or dowelled beams, as well as on that of connexions of various types which are subjected to forces.

7. Summary

The above fragmentary survey gives a general idea of the present state of knowledge concerning separate problems which relate to some essential aspects of the behaviour of load-bearing structures exposed to fires. At the same time, this paper states a series of urgent subjects for future structural fire engineering research.

This survey serves to illustrate the fact that the information available today affords a highly inadequate basis for reliable fire engineering design of load-bearing structures. Accordingly, emphasis is placed on the importance of rapid and intensive development of both theoretical and experimental research work in the field of structural fire engineering. Many of the urgent subjects for research which have been mentioned in the above are so extensive that it may be advantageous to tackle them at a collective inter-Scandinavian level or on a still wider international plane.

In the future treatment of the separate research problems of the type referred to in the above, an essential requirement is of course that they should not be regarded as independent subjects, but should be dealt with as significant stages of systematic long-range research programmes [72]. In the special case of load-bearing structures, this implies that the future results obtained from the studies of the various separate research problems should be combined so as to form the requisite basis for differentiated fire engineering design, which will enable the designer to take into account the factors involved in each individual case, such as the combustion characteristics of the fire load under consideration, the structural features of enclosed spaces, e.g. volume, surfaces bounding the space, window and door openings, etc., the radiation properties and thermal inertia characteristics of the structures enclosing the space and contained in it, the changes caused by heating in the strength and deformation properties of the structural materials concerned, and the stresses which occur in the load-bearing structures at any given instant of the process of fire development, including the forced temperature stresses, if any, which are caused by heating due to fire.

References

1. PETTERSSON, O. Betons brandstabilitet — inledningsanförande vid 4. Nordiske Betonforskningskongres i Aalborg 1962. (Stability of Concrete Exposed to Fire — Introductory Address at the 4th Inter-Scandinavian Concrete Research Congress, Aalborg, Denmark, 1962.) Nordisk Betong, 1963, No. 1, pp. 34—36.
2. ÖDEEN, K. Theoretical Study of Fire Characteristics in Enclosed Spaces. Division of Building Construction, Royal Institute of Technology, Bulletin No. 10, Stockholm, 1963.
3. KAWAGOE, K., SEKINE, T. Estimation of Fire Temperature-Time Curve in Rooms. Building Research Institute, Occasional Report No. 11, Tokyo, 1963.
4. KOLLBRUNNER, C. F. Ausbildung der Stahlkonstruktionen in Bezug auf die Feuersicherheit. Internationale Vereinigung für Brückenbau und Hochbau, Sechster Kongress, Vorbericht, Stockholm, 1960, pp. 449—456.
5. Brandteknisk klassificering, Statens Provningsanstalt. (Fire Grading, National Swedish Institute for Materials Testing.) Meddelande 66, Stockholm, 1964.
6. ESSUNGER, G., JOHANNESSON, P. Brandskydd (Fire Protection.) Byggkommentarer, Stockholm, 1961, pp. 261—276.
7. BOUÉ, P. Der Feuerschutz im Stahlhochbau. Berichte des Deutschen Ausschusses für Stahlbau, No. 21, Cologne, 1959.
8. GEILINGER, W., BRYL, S. Feuersicherheit der Stahlkonstruktionen, IV. Teil, Schweizer Stahlbauverband, Mitteilungen der Technischen Kommission, No. 22, Zürich, 1962.
9. PTCHÉLINTZEV, V. A. Etude du régime thermique des incendies dans le but de déterminer les limites de stabilité au feu à prescrire pour les éléments de construction. Institut Scientifique Central pour la recherche sur la prévention du feu, Moscou, 1958.
10. KOLLBRUNNER, C. F. Beurteilung der Feuersicherheit von Stahlhochbauten. Internationale Vereinigung für Brückenbau und Hochbau, Sechster Kongress, Schlussbericht, Stockholm, 1960, pp. 255—259.
11. FUJITA, K. Fire Research in Japan — Fire Spread Caused by Fire Radiant Heat and Methods of Prevention. Conseil International du Bâtiment pour la Recherche (CIB), GTF/FRWP, No. 32/J/1.
12. ÖDEEN, K. Teoretisk bestämning av temperaturförloppet i några av brand påverkade konstruktioner. (Theoretical Determination of Temperature Development in a Number of Constructions Subjected to Fire.) Byggmästaren, No. 4, 1963, and Division of Building Construction, Royal Institute of Technology, Bulletin No. 9, Stockholm, 1963.
13. YOKOI, S. Study of the Prevention of Fire-Spread Caused by Hot Upward Current. Building Research Institute, Report No. 34, Tokyo, 1960.
14. FAURE, J. Study of Convection Currents Created by Fires of Large Area. International Symposium on the Use of Models in Fire Research, Washington, 1961, pp. 130—147.
15. THOMAS, P. H. Some Studies of Models in Fire Research, VFDB (Vereinigung zur Förderung des Deutschen Brandschutzes) Zeitschrift, No. 3, Stuttgart, 1960, pp. 96—101.
16. FIRE RESEARCH 1960. Report of the Fire Research Board with the Report of the Director

of Fire Research, Department of Scientific and Industrial Research and Fire Offices' Committee Joint Fire Research Organization, Her Majesty's Stationery Office, London, 1961. Cf. also THOMAS, P. H., WEBSTER, C. T., RAFTERY, M. M. Some Experiments on Buoyant Diffusion Flames. Fire International, No. 2, October 1963, pp. 74—87.

17. GROSS, D. Experiments on the Burning of Cross Piles of Wood. Journal of Research of the National Bureau of Standards, Vol. 66, No. 2, April—June 1962, pp. 99—105.
18. WEBSTER, C. T., RAFTERY, M. M. The Burning of Fires in Rooms, Part II. Tests with Cribs in High Ventilation on Various Scales. Department of Scientific and Industrial Research and Fire Offices' Committee Joint Fire Research Organization, F. R. Note No. 401, 1959.
19. KAWAGOE, K. Fire Behaviour in Rooms. Building Research Institute, Report No. 27, Tokyo, 1958.
20. SIMMS, D. L., HIRD, D., WRAIGHT, H. G. H. The Temperature and Duration of Fires. Some Experiments with Models with a Restricted Ventilation. Department of Scientific and Industrial Research and Fire Offices' Committee Joint Fire Research Organization, F. R. Note No. 412, 1960.
21. ASHTON, L. A., MALHOTRA, H. L. External Walls of Buildings. Part I. The Protection of Openings against Spread of Fire from Storey to Storey. Department of Scientific and Industrial Research and Fire Offices' Committee Joint Fire Research Organization, F. R. Note No. 436, 1960.
22. HIRD, D., FISCHL, C. F. Fire Hazard of Internal Linings. Department of Scientific and Industrial Research and Fire Offices' Committee Joint Fire Research Organization, National Building Studies, Special Report No. 22, London, 1954.
23. RIEMANN, W. Die Erwärmung legierter Stähle in Abhängigkeit von Zusammensetzung, Abmessung und Lage im Ofen. Stahl und Eisen, No. 7, Düsseldorf, 1963, pp. 398—406.
24. SCHLYTER, R., ODEMARK, N. Brandsäkerheten hos vissa bjälklagskonstruktioner jämte teoretisk bestämning av brandtemperaturer uppkommande i byggnadskonstruktioner. Statens Provningsanstalt. (Fire Resistance of Some Floor Slab Structures and Theoretical Determination of Fire Temperatures Occurring in Building Structures. National Swedish Institute for Materials Testing.) Meddelande 65, Stockholm, 1935.
25. Eldfast murverk. (Fireproof Masonry.) Höganäs-Billesholms AB, 1933.
26. OTTOSON, G. Värmeledningstalets variation med temperaturen — litteratursammanställning. (Variation in Thermal Conductivity with Temperature — Review of Literature.) Stockholm, 1963.
27. According to investigations carried out at the Forschungsheim für Wärmeschutz, E. V., Munich, 1956. Cf. Rockwoolhandboken (Rockwool Manual), Section 6.
28. MANSERGH, R. A. Modern Thermal Insulating Practice. Journal of the Institution of Heating and Ventilating Engineers, June 1961.
29. JOACHIM, H. Feuerungs- und Schornsteinbau. Leipzig, 1953.
30. WILKES, B., WOOD, C. O. The Specific Heat of Thermal Insulating Materials. Transactions of the American Society of Heating and Ventilating Engineers, Vol. 48, 1942, p. 493.
31. HARMATHY, T. Z. A Treatise on Theoretical Fire Endurance Rating. National Research Council, Canada, Division of Building Research, Research Paper No. 153, Ottawa, 1962.

32. PERRY, J. H. Chemical Engineers' Handbook. Third Edition. New York-Toronto-London, 1950.

33. LJUNGGREN, P. Determination of Mineralogical Transformations of Gypsum by Differential Thermal Analysis. Journal of the American Ceramic Society, Vol. 43, 1960, p. 227.

34. WEST, R. R., SUTTON, W. J. Thermography of Gypsum. Journal of the American Ceramic Society, Vol. 37, 1954, p. 221.

35. KELLEY, K. K., SOUTHARD, J. C., ANDERSON, C. T. Thermodynamic Properties of Gypsum and its Dehydration Products. U. S. Department of Interior, Bureau of Mines, Technical Paper No. 625, 1941.

36. SCHMIDT, H., FURTHMANN, E. Über die Gesamtstrahlung fester Körper. Mitt. K.-Wilh.-Inst., Eisenforschg. 10, 1928. Cf. also e.g. GRÖBER, H., ERK, S., GRIGULL, U. Grundgesetze der Wärmeübertragung. Berlin—Göttingen—Heidelberg, 1961.

37. ROS, M., EICHINGER, A. Festigkeitseigenschaften der Stähle bei hohen Temperaturen. Eidg. Materialprüfungsanstalt an der ETH, Zürich, Bericht Nr. 87, 1934, and Bericht Nr. 138, 1941.

38. GEILINGER, E., GEILINGER, W. Feuersicherheit der Stahlkonstruktionen, II. Teil. Schweizer Stahlbauverband, Mitteilungen der Technischen Kommission, Heft 15, Zürich, 1956.

39. DANNEBERG, J., DEUTSCHMANN, H., MELCHIOR, P. Warmzerreissversuche mit Spannstählen und Auswertung von Brandversuchen an vorgespannten und nicht vorgespannten Stahlbetonbauteilen. Deutscher Ausschuss für Stahlbeton, Heft 122, Berlin, 1957.

40. SVENSKA TARIFFÖRENINGEN. Betong och brand. (Concrete and Fire.) Stockholm, 1959.

41. CUR (Commissie voor Uitvoering van Research ingesteld door de Betonvereniging). Brandproeven op voorgespannen betonliggers. Rapport 13, Den Haag, 1958.

42. Aktuella armeringsproblem. (Present-Day Reinforcement Problems.) Väg- och vattenbyggaren, No. 8, Stockholm, 1961, p. 291.

43. HERTEL, H. Leichtbau. Berlin—Göttingen—Heidelberg, 1960.

44. KREKEL, P., REICHEL, K. Aluminium-Legierungen für die Luftfahrt. Luftfahrttechnik, Bd. 2, 1956, No. 3, p. 45.

45. LEWIS, F. A. Aluminum-Base Materials. Engineering Materials Handbook, Section 6. New York—Toronto—London, 1958.

46. Aluminium-Taschenbuch, 11. Auflage. Düsseldorf, 1955.

47. PHILLEO, R. Some Physical Properties of Concrete at High Temperatures. Journal of the American Concrete Institute, Vol. 29, No. 10, April 1958, p. 857.

48. MALHOTRA, H. L. The Effect of Temperature on the Compressive Strength of Concrete. Magazine of Concrete Research, Vol. 8, No. 23, August 1956, p. 85.

49. BUSCH, H. Feuereinwirkung auf nicht brennbare Baustoffe und Baukonstruktionen. Berlin, 1938.

50. GRAF, O., ALBRECHT, W., SCHÄFFLER, H. Die Eigenschaften des Betons. Berlin—Göttingen—Heidelberg, 1960, p. 167.

51. LEHMANN, N., MÄLZIG, G. Über die Heissdruckfestigkeit von Beton. Tonindustrie-Zeitung, 1960, p. 414.

52. FIRE RESEARCH 1957. Report of the Fire Research Board and the Report of the Director of Fire Research, Department of Scientific and Industrial Research and Fire Offices' Committee Joint Fire Research Organization, Her Majesty's Stationery Office, London, 1958.

53. CARLSON, C. C., BENJAMIN, I. A., SHERIDAN, R. R., TROXELL, G. E. Symposium on Fire

Resistance of Concrete. American Concrete Institute, Special Publication, SP-5 1962.

54. KORDINA, K. Das Verhalten von Stahlbeton- und Spannbetonbauteilen unter Feuerangriff. Institut für Baustoffkunde der Technischen Hochschule, Braunschweig, Heft 2, February, 1963.
55. NEKRASSOW, K. D. Hitzebeständiger Beton. Wiesbaden—Berlin, 1961.
56. ENGWALL, A. Fire Resistance of Siporex Products. RILEM, Proceedings of the Symposium on Light-Weight Concrete held in Göteborg 1960, Göteborg, 1961, p. 553.
57. BAEHR, H. D. Wärmeleitung. Handbuch der Kältetechnik, Dritter Band. Berlin—Göttingen—Heidelberg, 1959, pp. 98—184.
58. CARSLAW, H. S., JAEGER, J. C. Conduction of Heat in Solids, Second Edition. Oxford, 1959.
59. GEBHART, B. Heat Transfer. New York—Toronto—London, 1961.
60. GRÖBER, H., ERK, S., GRIGULL, U. Die Grundgesetze der Wärmeübertragung, Dritte Auflage. Berlin—Göttingen—Heidelberg, 1961.
61. HIRSCHFELD, K. Die Temperaturverteilung im Beton. Berlin—Göttingen—Heidelberg, 1948.
62. JAKOB, M. Heat Transfer. Vol. I, New York—London, 1949, Vol. II, New York—London, 1957.
63. LYKOV, A. V., MIKHAYLOV, Y. A. Theory of Energy and Mass Transfer. Prentice-Hall, N. J., 1961.
64. SAWADA, M. On the General Solution of the Basic Equation of Thermal Conduction. — Problems of Thermal Conduction in One Dimension in Bodies with Varying Conductivities by Duhamel's Method. — On the General Solution of the Fundamental Equation of Thermal Conduction in Bodies whose Thermal Coefficients Are Affected by Temperature. National Research Council of Canada, Technical Translation 895—897, Ottawa, 1960.
65. Protection of Structural Steel Against Fire. Joint Fire Research Organization, Her Majesty's Stationery Office, Fire Note No. 2, London, 1961.
66. FUJII, S. The Theoretical Calculation of Temperature-Rise of Thermally Protected Steel Column Exposed to the Fire. Building Research Institute, Occasional Report No. 10, Tokyo, 1963.
67. PETTERSSON, O. Utvecklingstendenser rörande brandteknisk dimensionering av stålkonstruktioner. (Trends of Development in Fire Engineering Design of Steel Structures.) Väg- och vattenbyggaren, No. 6—7, Stockholm, 1964, p. 265.
68. THOMAS, F. G., WEBSTER, C. T. Investigation on Building Fires, Part VI, The Fire Resistance of Reinforced Concrete Columns. National Building Studies, Research Paper No. 18, Her Majesty's Stationery Office, London, 1953.
69. TENNING, K. Brandförsök med limmade träbalkar. (Fire Tests on Glued Timber Beams.) Väg- och vattenbyggaren, No. 2, Stockholm, 1961, p. 55.
70. IMAIZUMI, K. Stability in Fire of Protected and Unprotected Glued Laminated Beams. Norsk Treteknisk Institutt, Meddelelse Nr 18, Blindern, May 1962.
71. Träkonstruktioners brandstabilitet — symposium vid Chalmers Tekniska Högskola den 18 juni 1962. (Stability of Timber Structures Exposed to Fires — Symposium at the Chalmers University of Technology, June 18th, 1962.) Transactions of Chalmers University of Technology, Gothenburg, Sweden, No. 274, Göteborg, 1963.
72. PETTERSSON, O. General Programme for Scandinavian Long-Term Fire Engineering Research. Proceedings No. 129 of the National Swedish Institute for Materials Testing, Stockholm, 1963.

ELANDERS BOKTRYCKERI AKTIEBOLAG, GÖTEBORG 1968